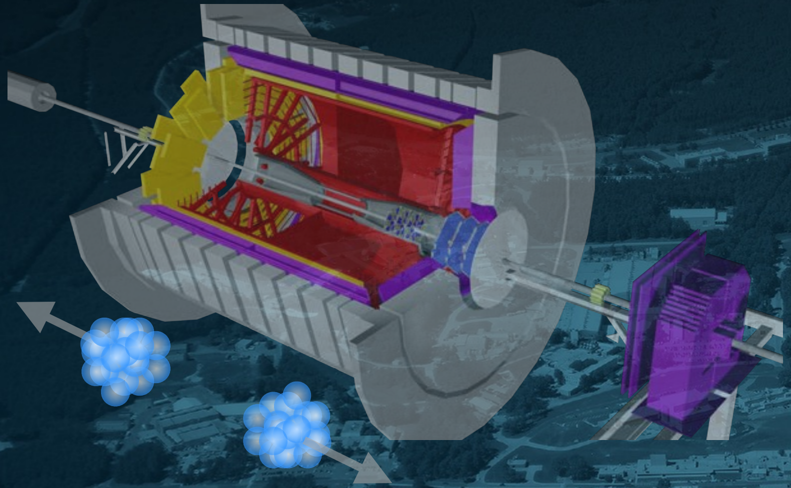

Brookhaven National Laboratory

U.S. DEPARTMENT OF ENERGY

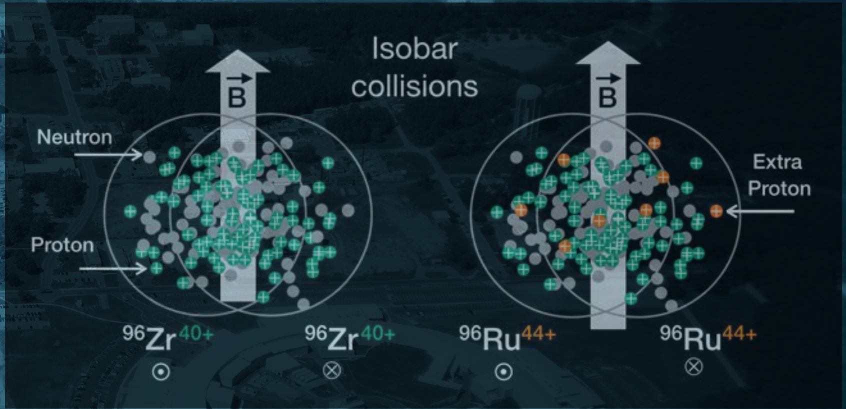


# Opportunities with the isobar run at RHIC

Prithwish Tribedy (Brookhaven National Laboratory)

Intersection of nuclear structure and high-energy nuclear collisions, week 3, Feb 6-10, 2023, INT, Seattle

# Opportunities with the isobar run at RHIC

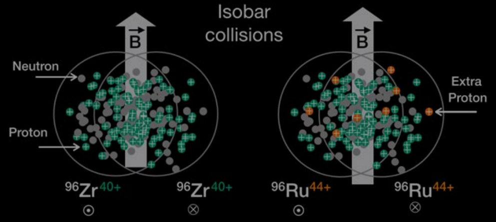


- Brief intro to our field & Isobar collisions at RHIC
  - Precision tool for measurements in heavy ion

- Nuclear shape and structure
  - Nuclear deformation, neutron skin

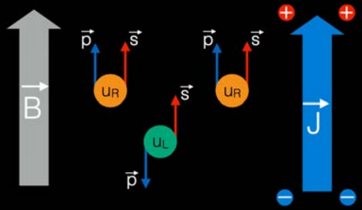


- Strong field effects
  - Photon-induced processes, Chiral Magnetic Effect, Polarization
- Study of the structure of a baryon
  - What exactly carries baryon quantum number and how is it stopped?

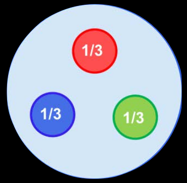


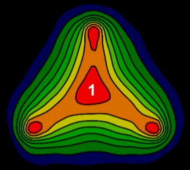

# Relativistic collisions are different

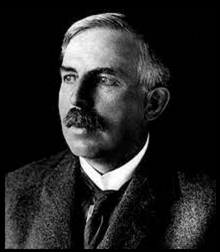

Rutherford, 1908

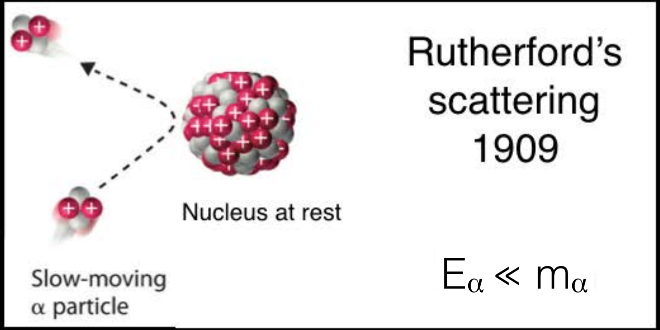


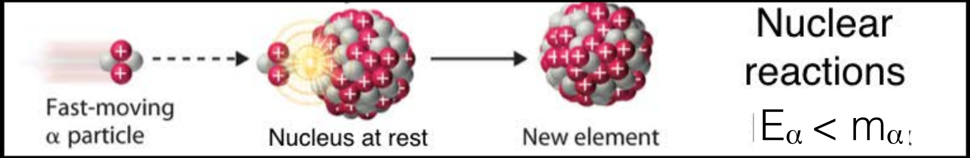


Lee, 1974

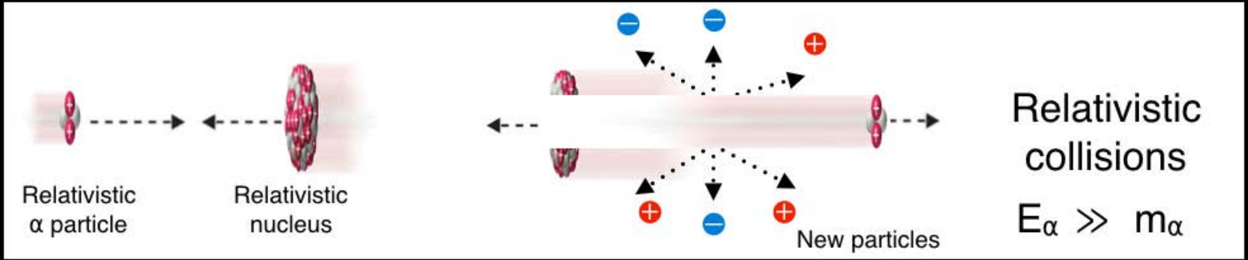


Relativistic collisions are very different as many new degrees of freedom appear after the collisions purely from quantum fluctuations

Study the building blocks of strong interaction & underlying QFT (typical time scales ~1-10 fm)

# Creation of strong color fields

Gribov, Levin, Ryskin, 1981
McLerran, Venugopalan
hep-ph/9309289

Expected to produce the strongest color field in the nature: $\rho \sim 1/\alpha_S$

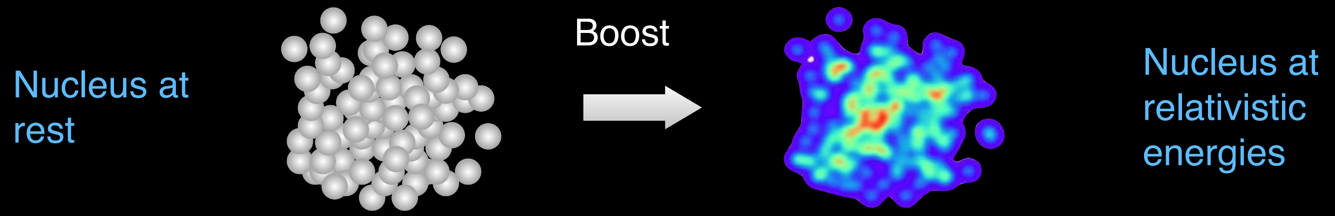


A state-of-the art modeling of heavy-ion collisions based on strong color fields is highly successful

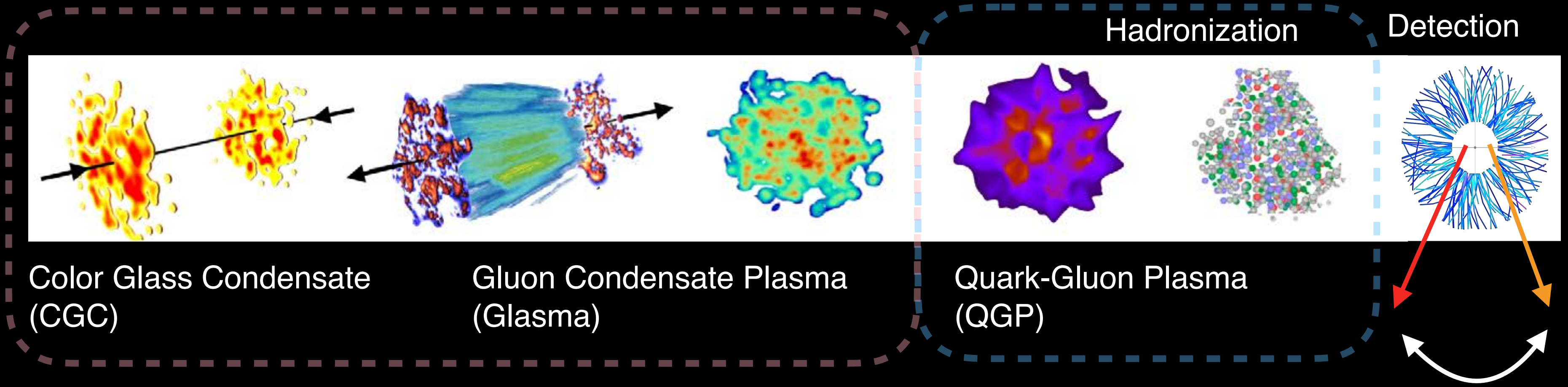

# Creation of strong electro-magnetic fields

Strongest EM field in the nature: $B\sim10^{18}$ Gauss (~ pion-mass$^2$)

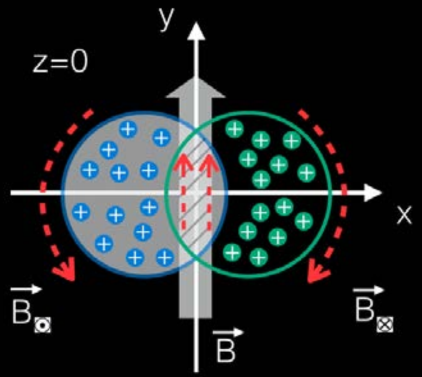


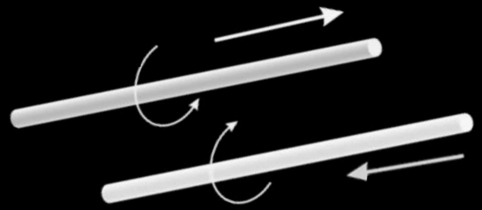

Kharzeev et al 0711.0950, Skokov et al 0907.1396 McLerran, Skokov, 1305.0774

Earth
~0.5 Gauss

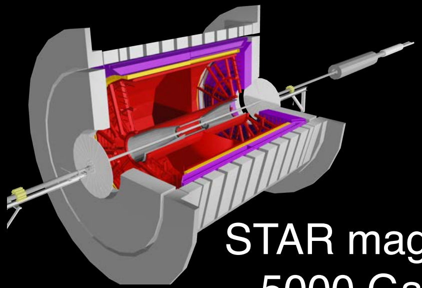

STAR magnet
~ 5000 Gauss

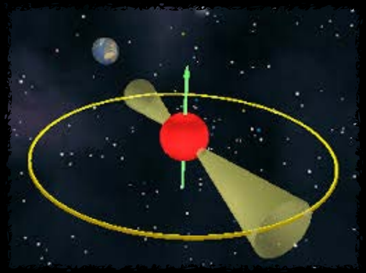

Neutron Star
~ $10^9$ Gauss

# The STAR detector at the Relativistic Heavy Ion Collider

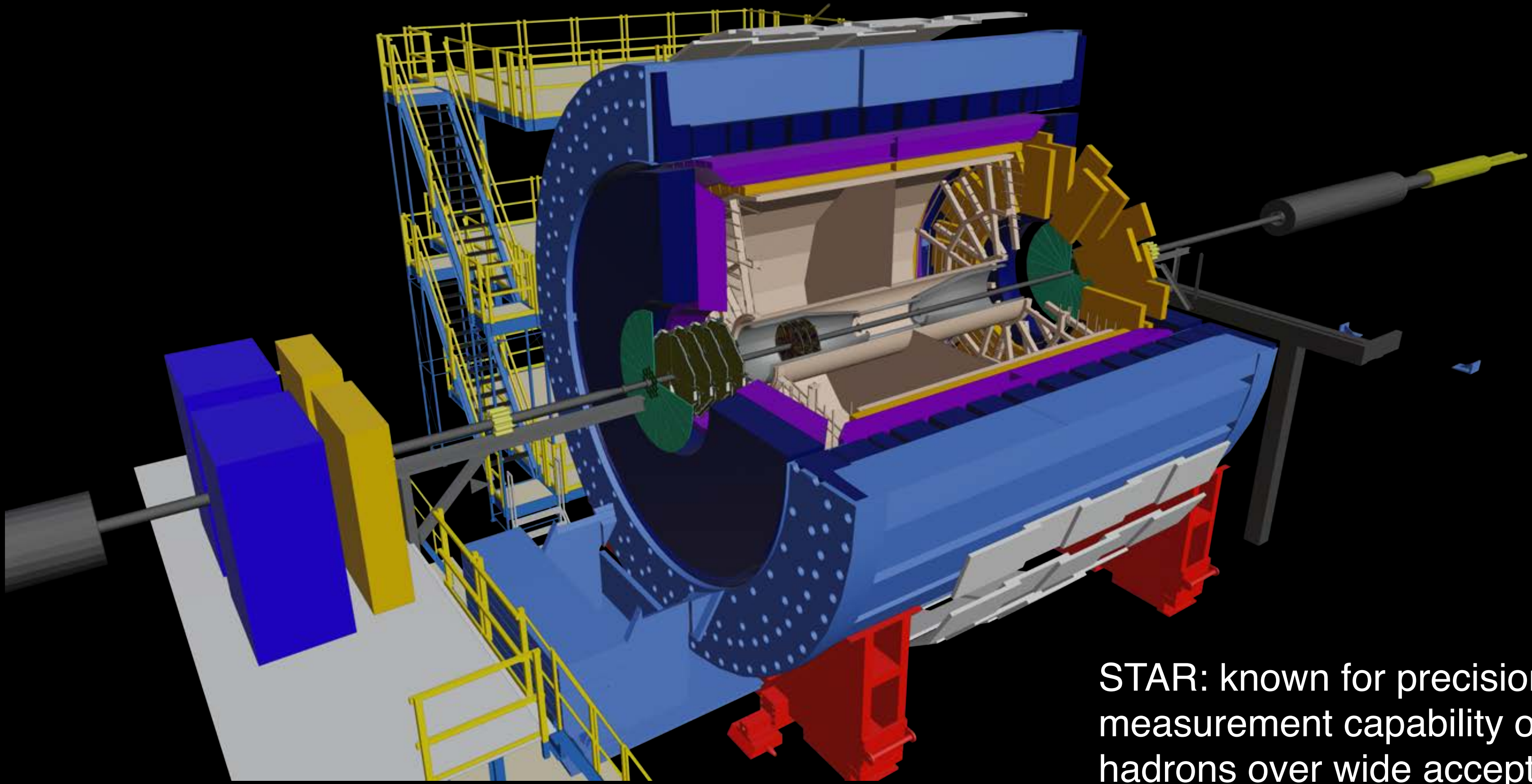

STAR: known for precision measurement capability of hadrons over wide acceptance

# A gold-gold collision @ STAR detector

https://www.star.bnl.gov/~dmitry/edisplay/

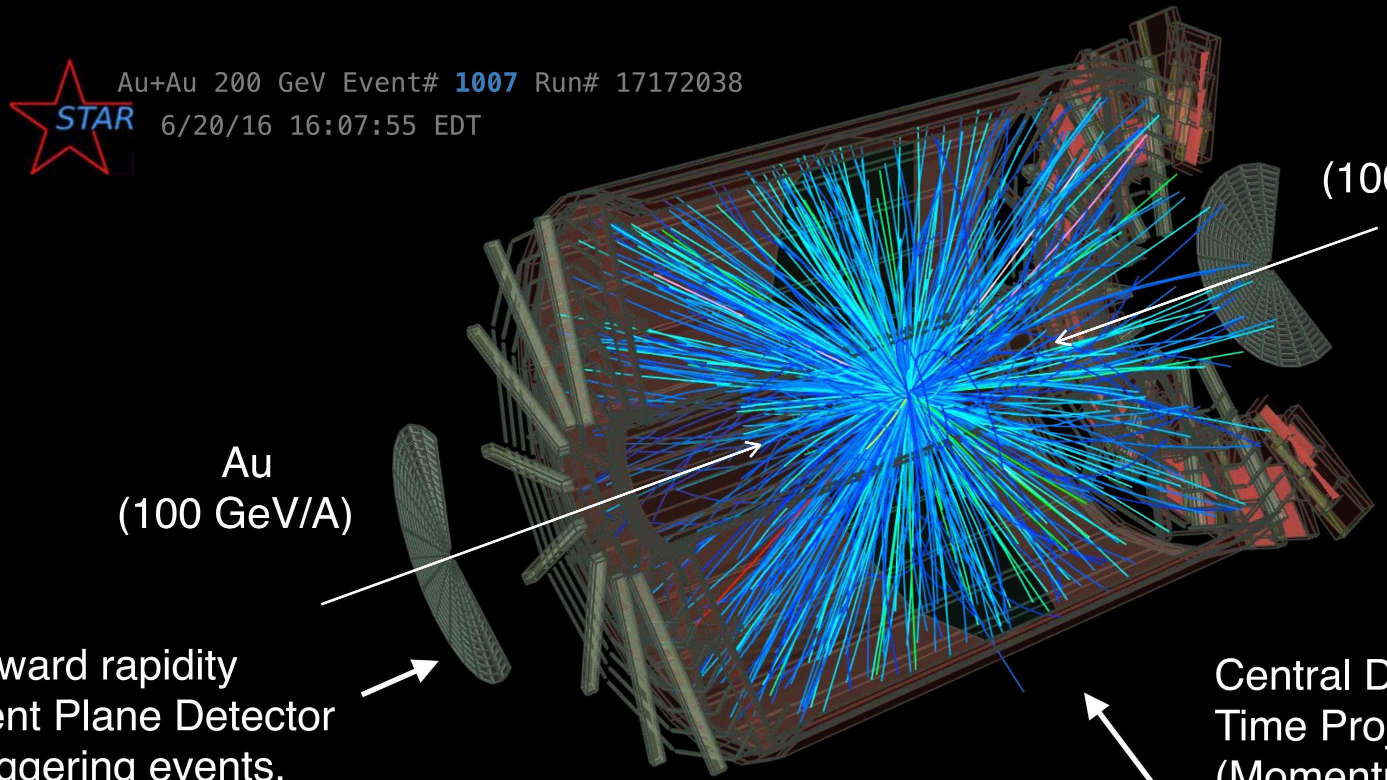


Forward rapidity
Event Plane Detector
(Triggering events,
plane of collisions)

Direction B-field

Central Detector (mid-rapidity)
Time Projection Chamber
(Momentum, charge state,
particle identification)

Motion of the charge

# Elliptic anisotropy in particle production

Elliptic anisotropy is measured by correlation between two particles

$$v_2\{EP\} = \langle \cos(2\phi_1 - 2\Psi_2) \rangle$$

$$v_2\{2\}^2 = \langle \cos(2\phi_1 - 2\phi_2) \rangle$$

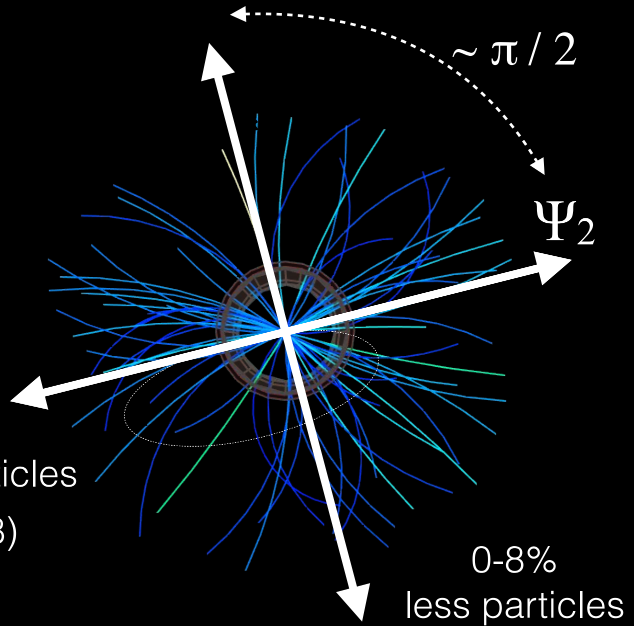


Distribution of particles look elliptic in every event: major axis is elliptic anisotropy plane $\Psi_2$

# Elliptic anisotropy in particle production

Elliptic anisotropy is measured by correlation between two particles

$$v_2\{EP\} = \langle \cos(2\phi_1 - 2\Psi_2) \rangle$$

$$v_2\{2\}^2 = \langle \cos(2\phi_1 - 2\phi_2) \rangle$$

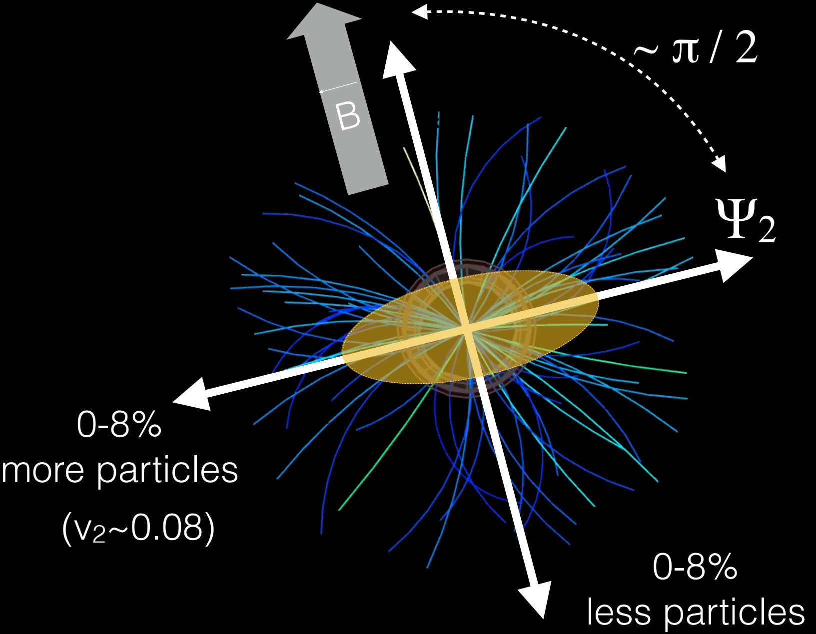


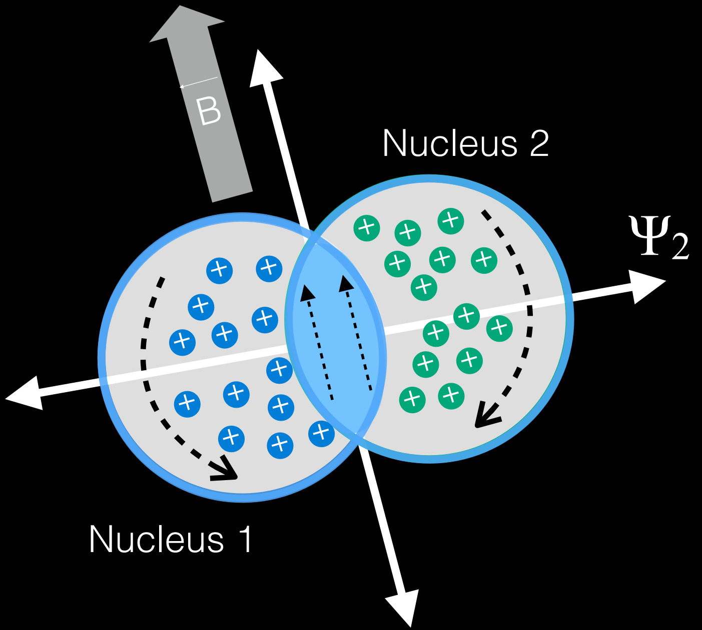


Distributions of particles look elliptic in every event: major axis is elliptic anisotropy plane $\Psi_2$

The plane of elliptic anisotropy $\Psi_2$ is correlated to B-field direction

# Higher order anisotropy

Quantify anisotropy using Fourier expansion: $$\frac{dN}{d\phi} = \frac{N}{2\pi}\left(1 + \sum_n 2v_n \cos(\phi - \Psi_n)\right)$$

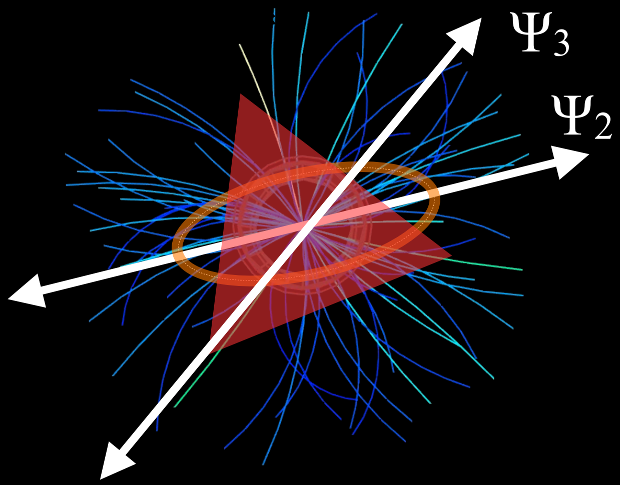


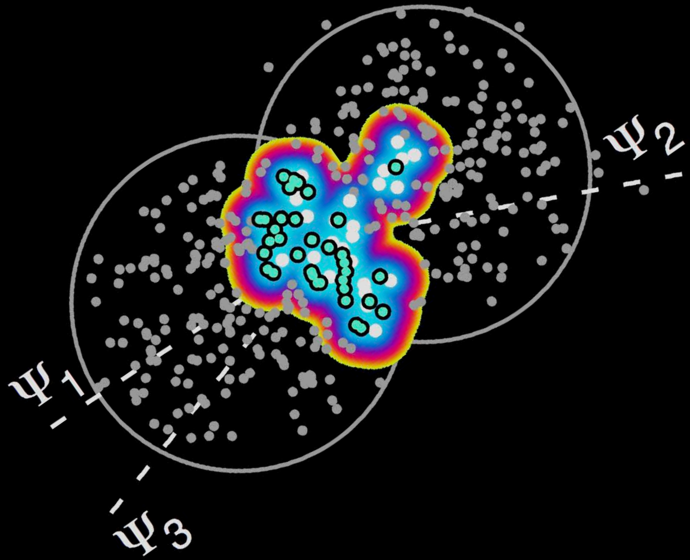


Particle distribution reveal various anisotropy coefficients & plane $\Psi_n$

Different harmonic anisotropies along $\Psi_n$ (generated due to initial state geometry + fluctuations)

# Centrality of collisions

b~0

b<2R

b>2R

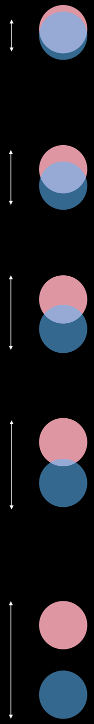

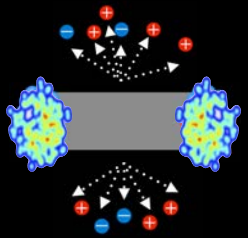

Central collisions
Strong process dominate

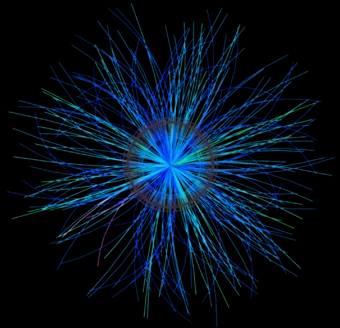

Nuclear
Deformation
studies

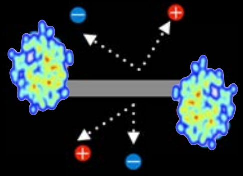

Peripheral collisions
Strong process dominate

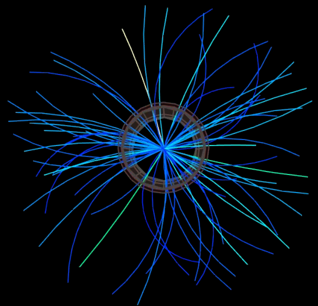

Chiral effects,
Polarization
Neutron skin

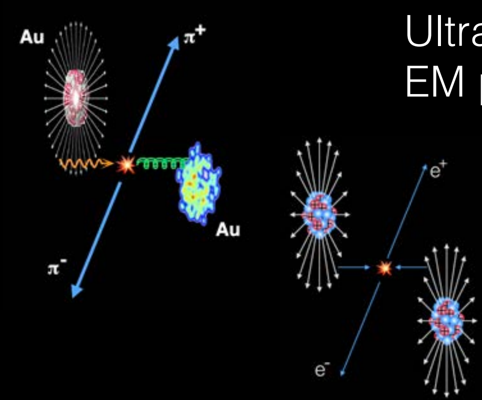


Ultra-peripheral collisions
EM process dominate

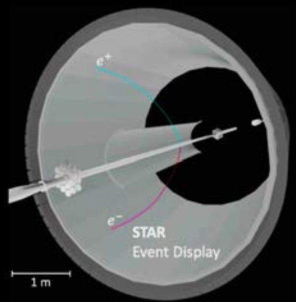


EM-field driven
effects, tomography
with polarized photon

# Isobar in the chart of nuclides

Elements with similar sizes but different protons so that B-field could be different

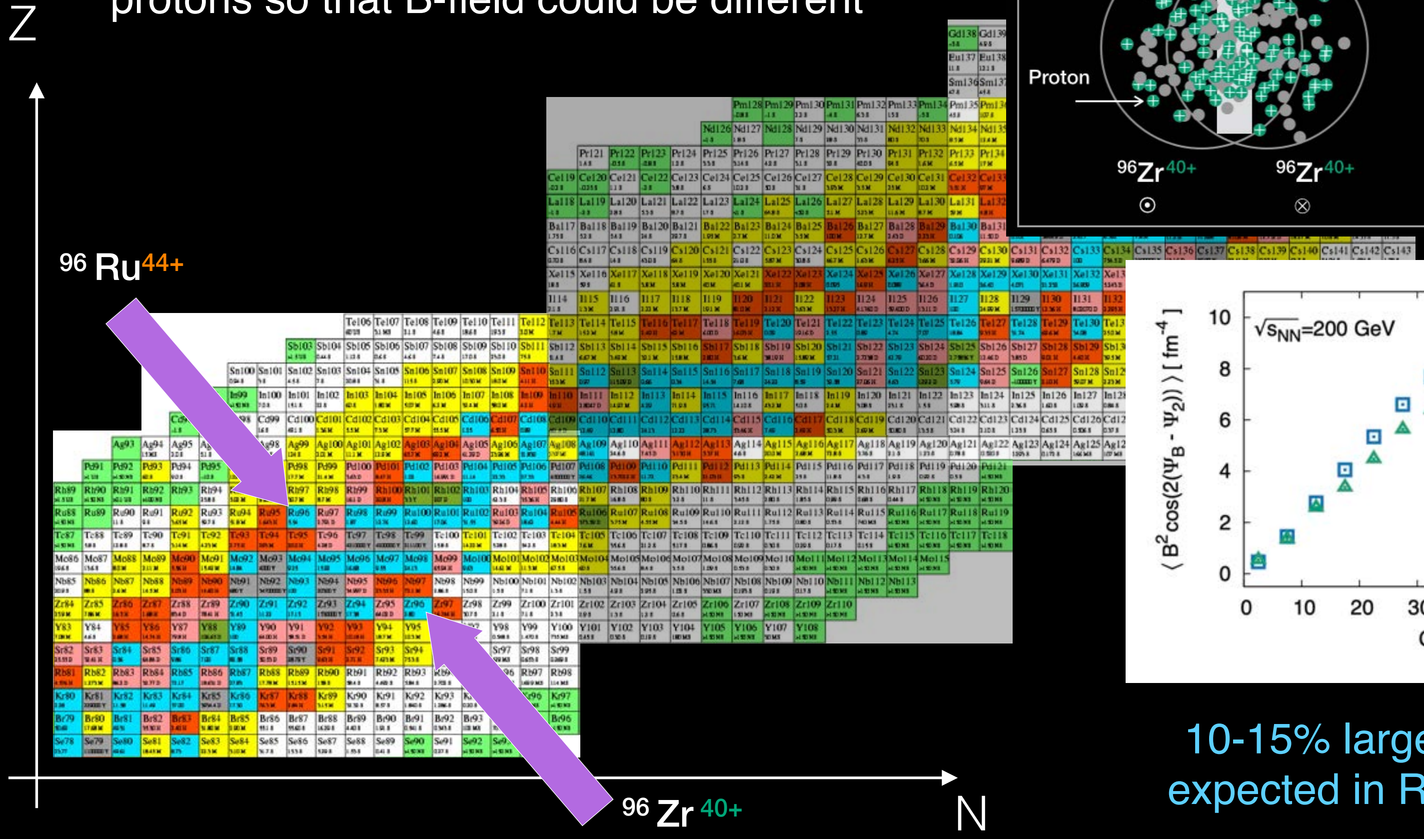


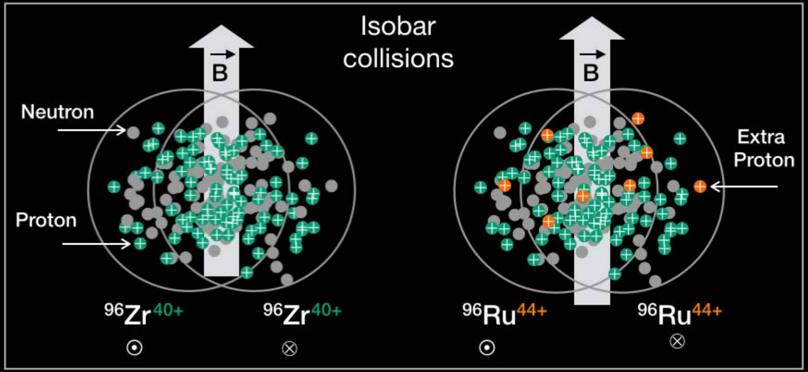


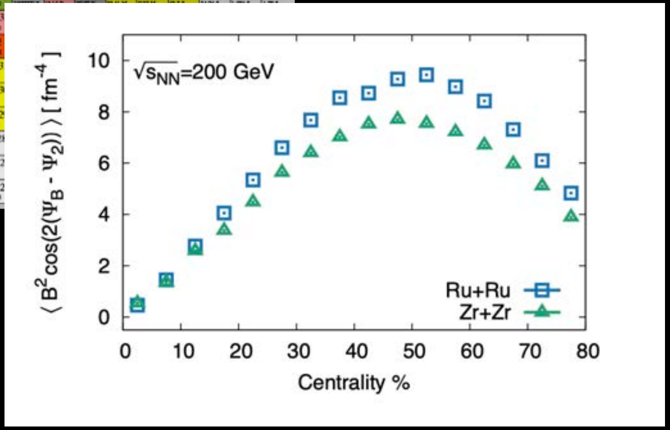


10-15% larger B-field square expected in Ru+Ru than Zr+Zr

# Isobar collisions at RHIC

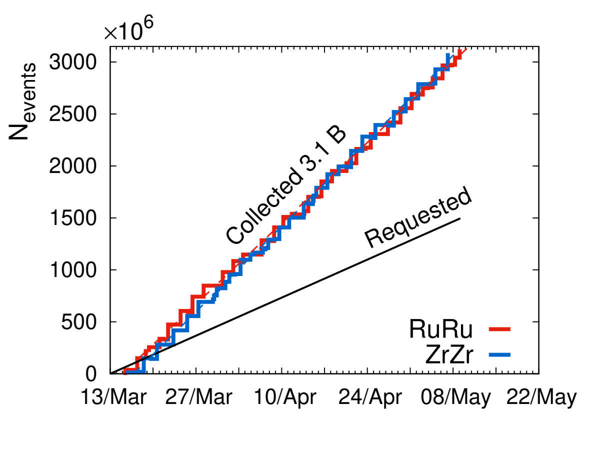


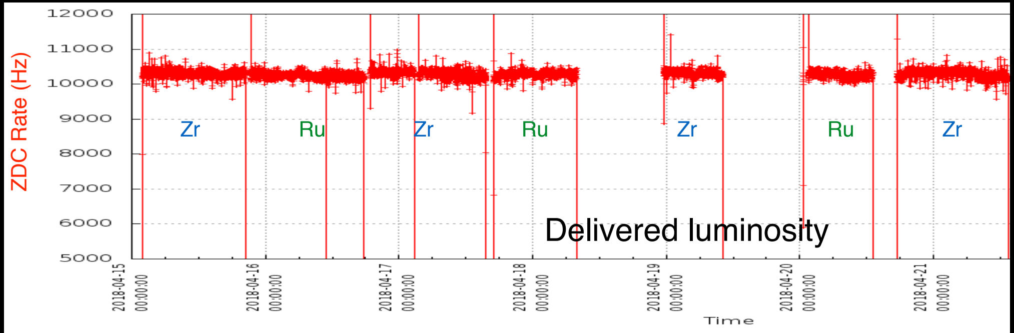


Special run to minimize systematics by:

1) Fill-by-fill switching
2) Level luminosity

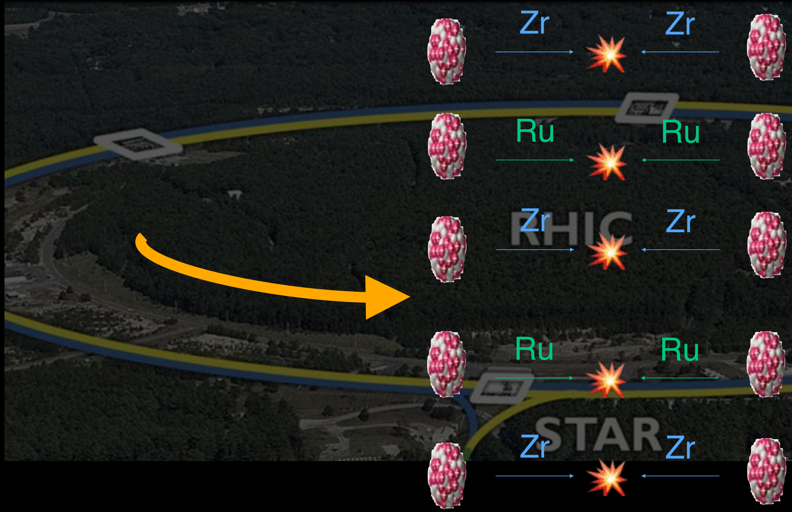


$$\frac{\langle \text{Observable} \rangle_{\text{Ru+Ru}}}{\langle \text{Observable} \rangle_{\text{Zr+Zr}}} \neq 1$$

Provides a unique way to improve precision to reduce systematics in any observable ratio

# Isobar program at RHIC: journey from 2018 to 2021

**Relativistic Heavy Ion Collider Begins 18th Year of Experiments**

First smashups with 'isobar' ions and low-energy gold-gold collisions will test earlier hints of exciting discoveries as accelerator physicists tune up technologies to enable future science

March 21, 2018

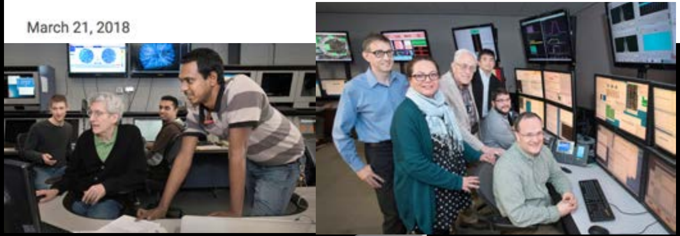

2018

2019

2020

2021

**Results from Search for 'Chiral Magnetic Effect' at RHIC**

Collisions of 'isobars' test effect of magnetic field, searching for signs of a broken symmetry

August 31, 2021

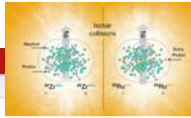

arXiv.org > nucl-ex > arXiv:2109.00131

Nuclear Experiment

[Submitted on 1 Sep 2021]

**Search for the Chiral Magnetic Effect with Isobar Collisions at $\sqrt{s_{NN}}$ = 200 GeV by the STAR Collaboration at RHIC**

STAR Collaboration: M. S. Abdallah, B. E. Aboona, J. Adam, L. Adamczyk, J. R. Adams, J. K. Adkins, G. Agakishiev, I. Aggarwal, M. M. Aggarwal, Z. Ahammed, I. Alekseev, D. M. An
Ashraf, F. G. Atetalla, A. Attri, G. S. Averichev, V. Bairathi, W. Baker, J. G. Ball Cap, K. Barish, A. Behera, R. Bellwied, P. Bhagat, A. Bhasin, J. Bielcik, J. Bielcikova, I. G. Bordyuzhin, J.
X. Z. Cai, H. Caines, M. Calderón de la Barca Sánchez, D. Cebra, I. Chakaberia, P. Chaloupka, B. K. Chan, F-H. Chang, Z. Chang, N. Chankova-Bunzarova, A. Chatterjee, S. Chattop
Chen, Z. Chen, J. Cheng, M. Chevalier, S. Choudhury, W. Christie, X. Chu, H. J. Crawford, M. Csanád, M. Daugherity, T. G. Dedovich, I. M. Deppner, A. A. Derevschikov, A. Dhamija
J. L. Drachenberg, E. Duckworth, J. C. Dunlop, N. Elsey, J. Engelage, G. Eppley, S. Esumi, O. Evdokimov, A. Ewigleben, O. Eyser, R. Fatemi, F. M. Fawzi, S. Fazio, P. Federic, J. Fedori
Fisyak, A. Francisco,

Search for the chiral magnetic effect with isobar collisions at $\sqrt{s_{NN}} = 200$ GeV by the STAR Collaboration at the BNL Relativistic Heavy Ion Collider

M. S. Abdallah *et al.* (STAR Collaboration)
Phys. Rev. C **105**, 014901 – Published 3 January 2022

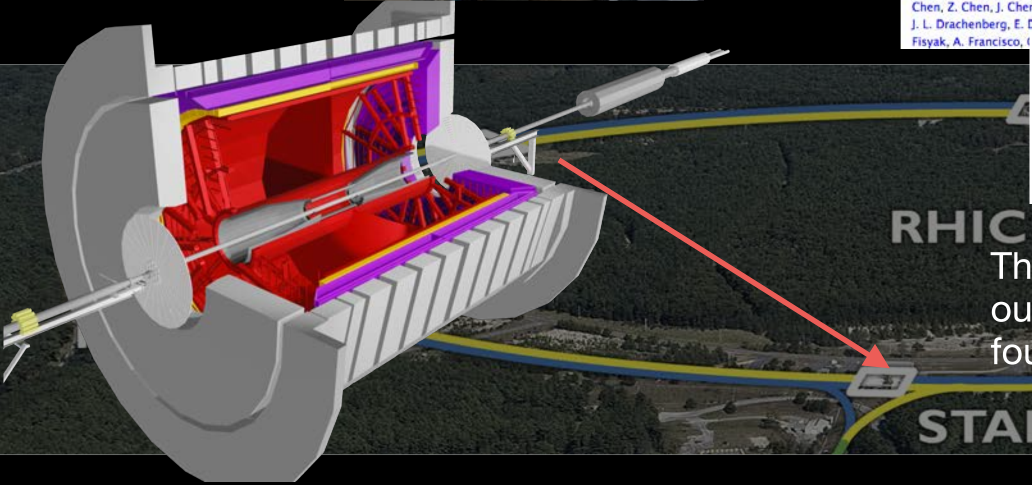


The published results were outcome of blind analysis from four independent groups

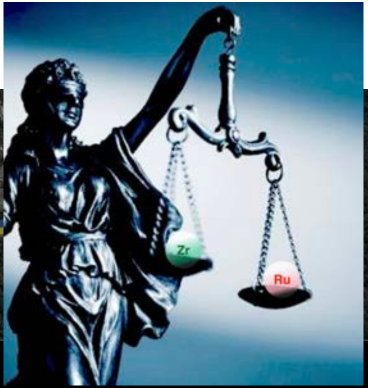


The versatility of RHIC and the unique capabilities of the STAR detector were crucial to the success of the isobar program

# Insights on nuclear shape & structure

# Multiplicity difference between the isobars

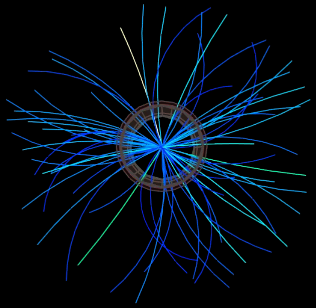

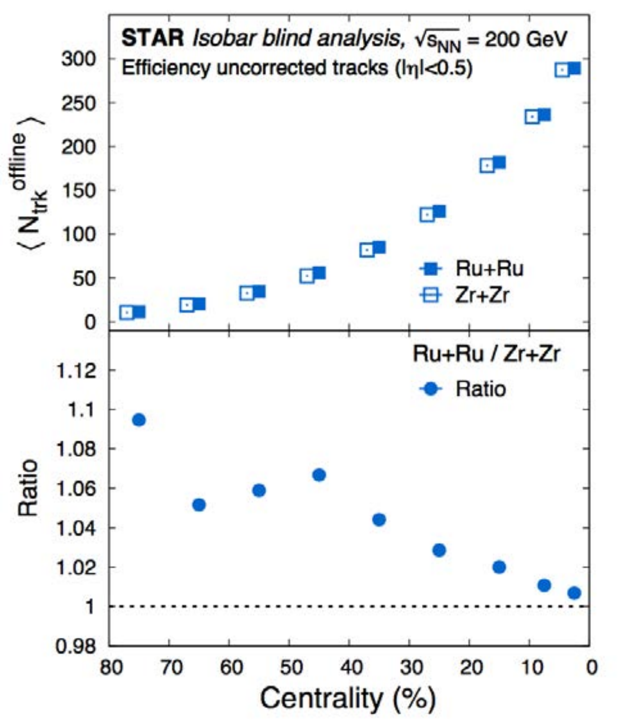


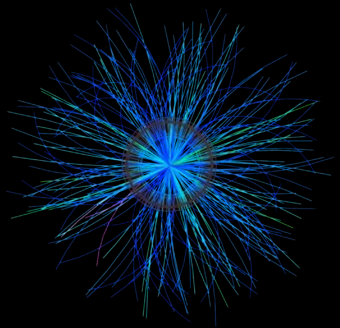

Xu et. al., Phys. Rev. Lett. 121, 022301 (2018)

| | Case-3 [113] | | |
|---|---|---|---|
| Nucleus | $R$ (fm) | $a$ (fm) | $\beta_2$ |
| $^{96}_{44}$Ru | 5.067 | 0.500 | 0 |
| $^{96}_{40}$Zr | 4.965 | 0.556 | 0 |

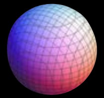

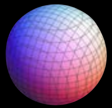

Multiplicity density is larger in Ru than in Zr in a matching centrality

Indicates smaller size of the Ru nucleus than Zr

# Multiplicity difference between the isobars

| Nucleus | Case-1 [83] $R$ (fm) | $a$ (fm) | $\beta_2$ |
|---|---|---|---|
| $^{96}_{44}$Ru | 5.085 | 0.46 | 0.158 |
| $^{96}_{40}$Zr | 5.02 | 0.46 | 0.08 |

| Nucleus | Case-2 [83] $R$ (fm) | $a$ (fm) | $\beta_2$ |
|---|---|---|---|
| $^{96}_{44}$Ru | 5.085 | 0.46 | 0.053 |
| $^{96}_{40}$Zr | 5.02 | 0.46 | 0.217 |

| Nucleus | Case-3 [113] $R$ (fm) | $a$ (fm) | $\beta_2$ |
|---|---|---|---|
| $^{96}_{44}$Ru | 5.067 | 0.500 | 0 |
| $^{96}_{40}$Zr | 4.965 | 0.556 | 0 |

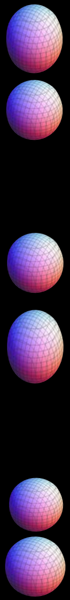

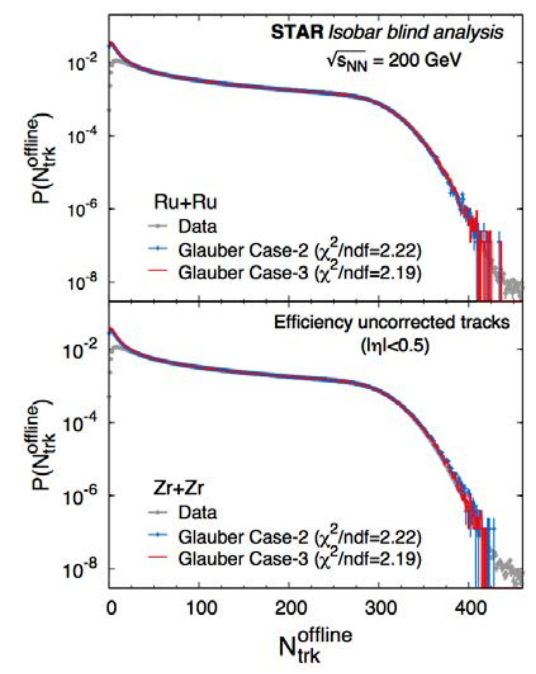


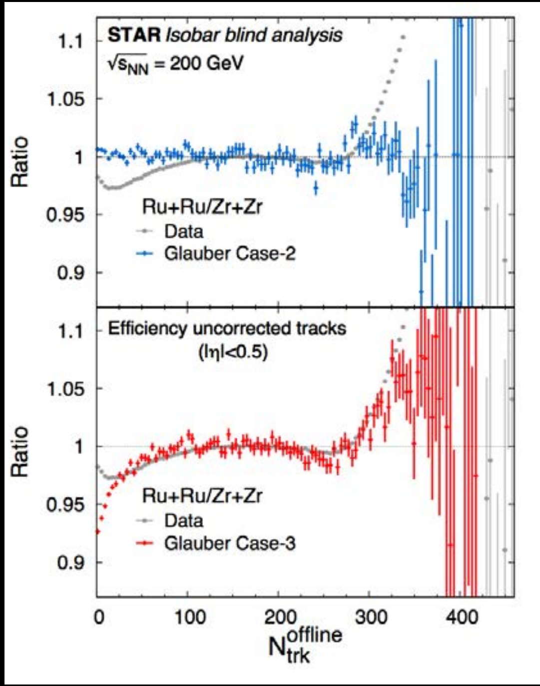


Deng et. al., Phys. Rev. C 94, 041901 (2016),
Xu et. al., Phys. Rev. Lett. 121, 022301 (2018)

MC-Glauber with two-component model used to describe uncorrected multiplicity distribution.
WS parameters with thinker neutron skin in Zr provides the best description of the multiplicity distributions

# Nuclear structure difference between isobars

Talk by Haojie Xu (Week 2)

Multiplicity distribution $P(N_{ch})$ and net-charge multiplicity ($\Delta Q$) indicate neutron skin difference

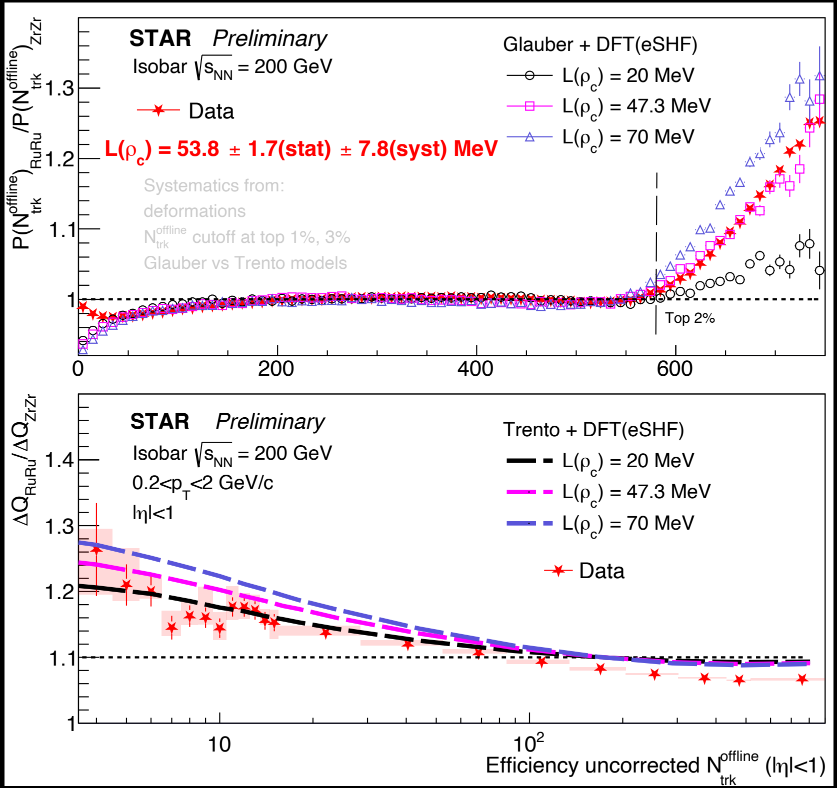


Ru+Ru

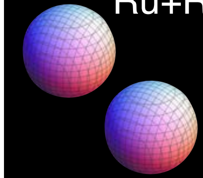

Zr+Zr

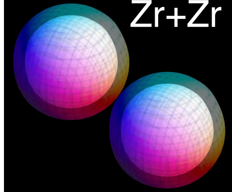

Neutron skin:

$\Delta r_{np}$ (Zr) > $\Delta r_{np}$(Ru)

Pioneering new ways to constrain neutron skin with heavy ion collisions

# Measurements of elliptic anisotropy

$$v_2\{EP\} = \langle \cos(2\phi_1 - 2\Psi_2) \rangle \quad v_2\{2\}^2 = \langle \cos(2\phi_1 - 2\phi_2) \rangle$$

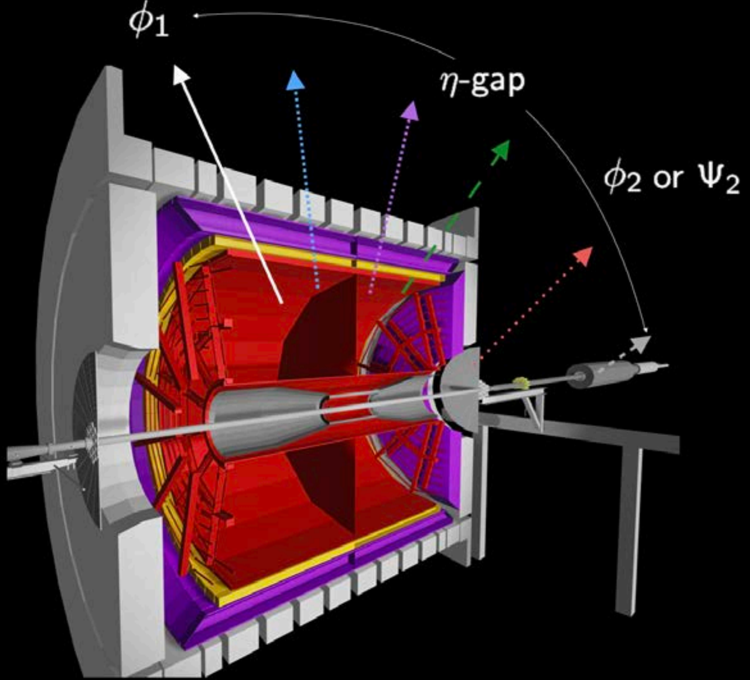


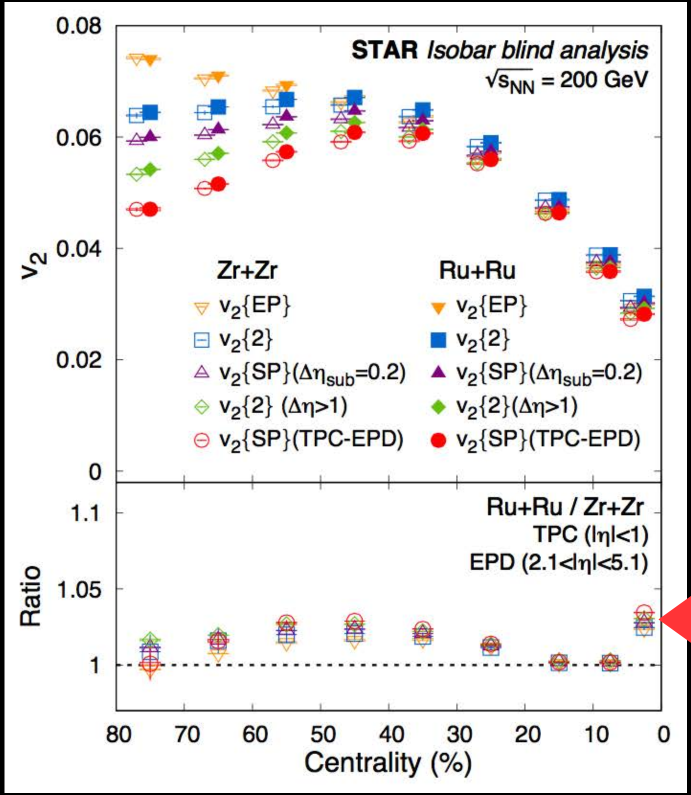


$v_2$ ratio is greater than unity indicating shape difference between two isobars (larger quadruple deformation in Ru)

# Measurements of triangular anisotropy

$$v_3\{2\}^2 = \langle \cos(3\phi_1 - 3\phi_2) \rangle$$

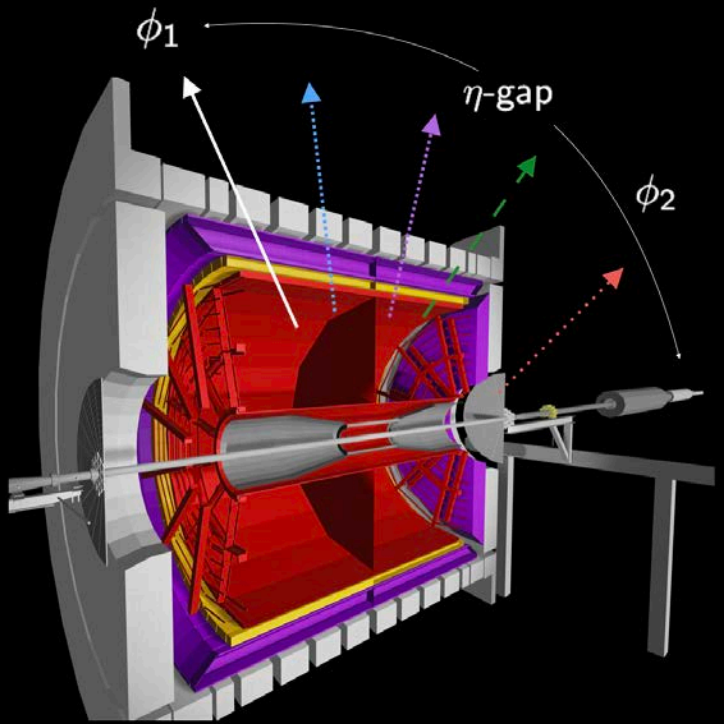


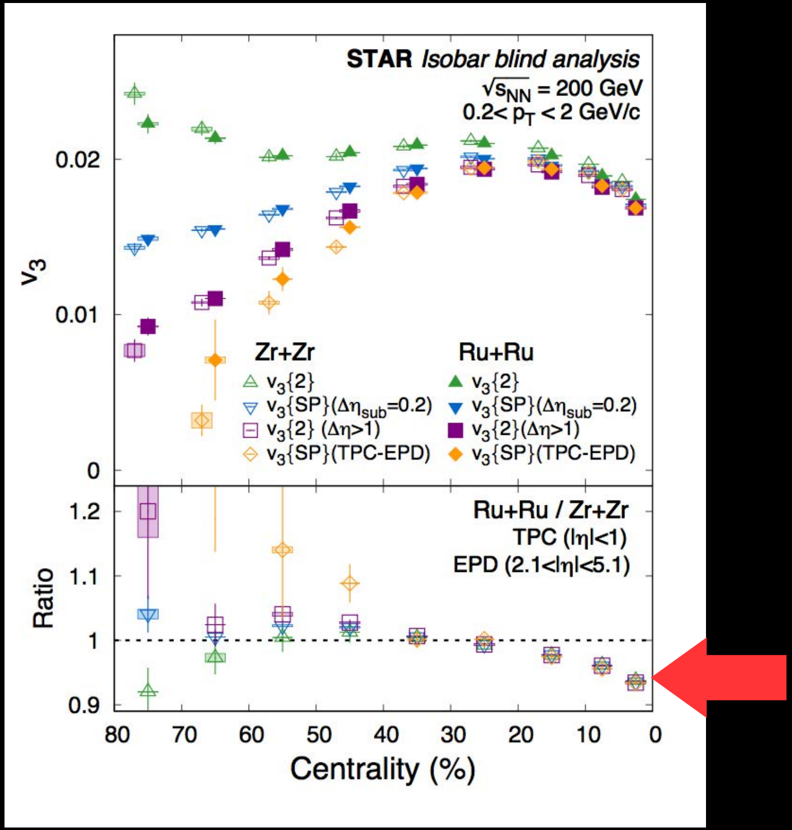


$v_3$ ratio is smaller than unity indicating shape difference between two isobars (larger octuple deformation in Zr)

# Measurements of mean transverse momentum

$$\delta p_T = p_T - [p_T]$$

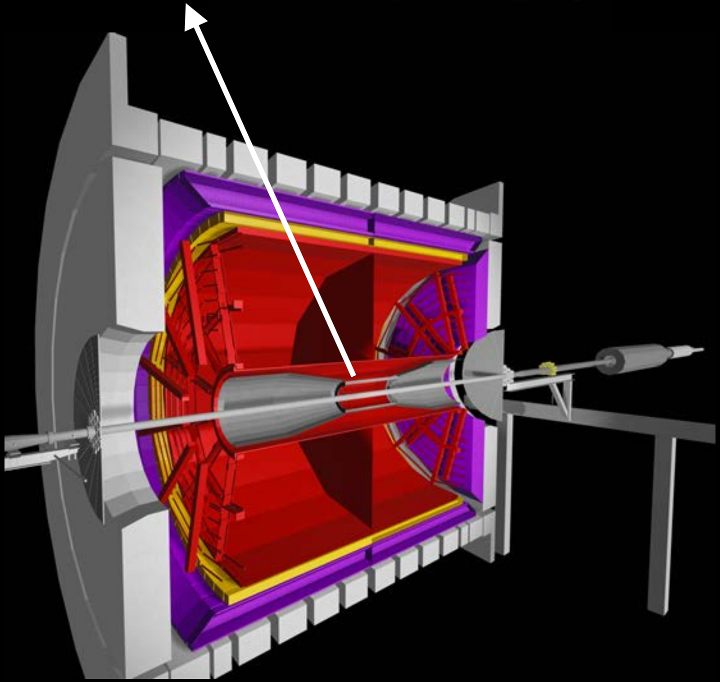

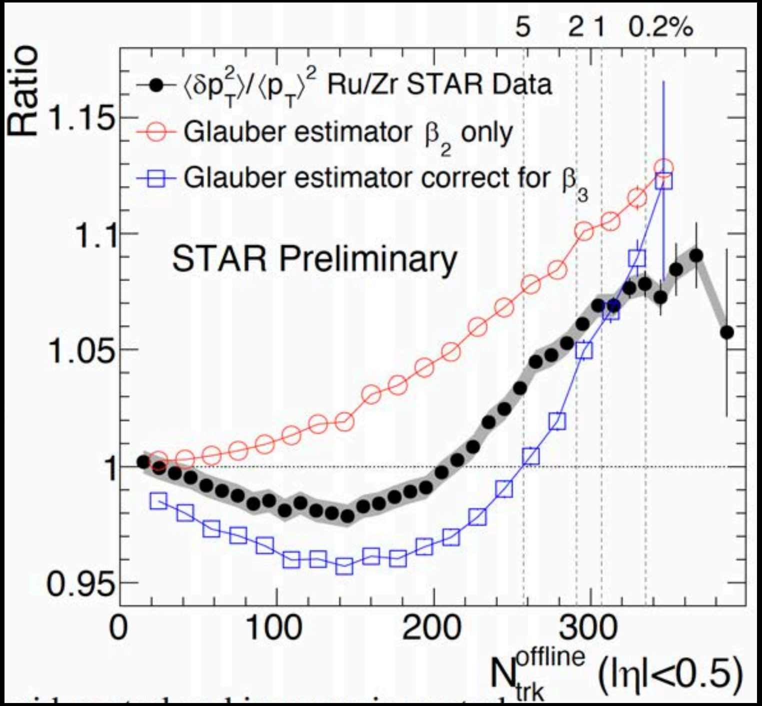


Transverse pT

# Nuclear structure difference between isobars

**Talk by Giuliano Giacalone, Chunjian Zhang (week 3), Jiangyong Jia (week 2)**

Ratios of flow harmonics ($v_2$, $v_3$), $<p_T>$ fluctuations indicate nuclear shape difference between isobars

**Giacalone, Phys. Rev. Lett. 124, 202301 (2020)**

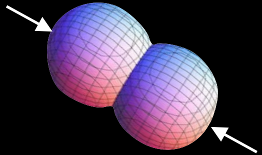

No deformation (Baseline)

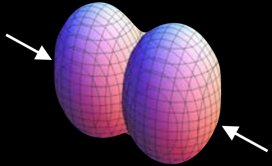

Side-Side prolate

Large $v_2$ & low $\langle p_T \rangle$

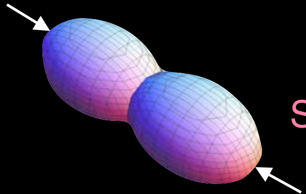

Tip-Tip prolate

Small $v_2$ & high $\langle p_T \rangle$

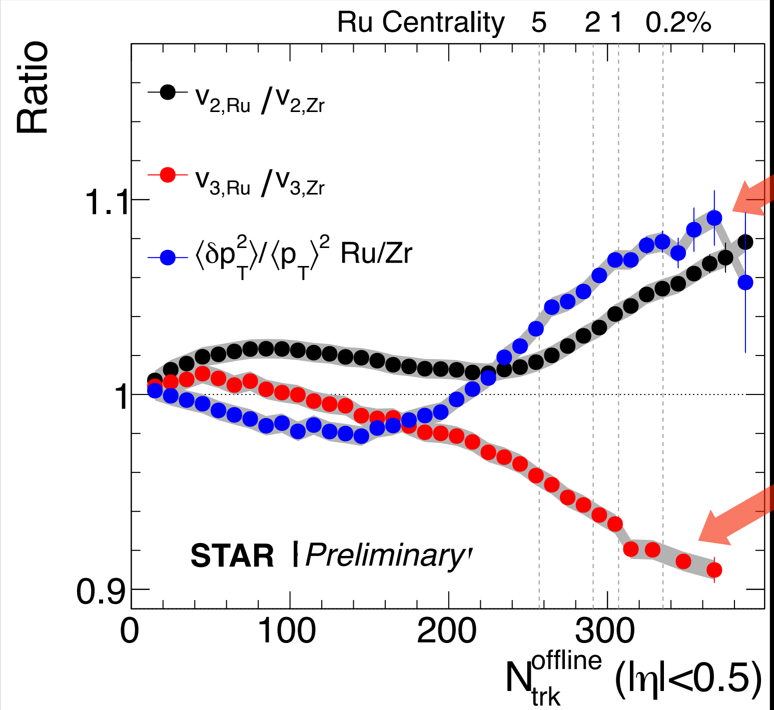


Ru+Ru

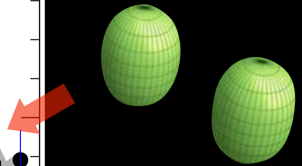

Zr+Zr

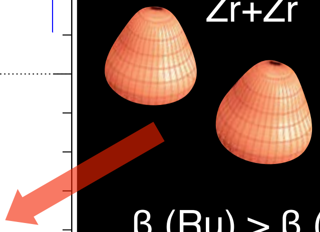

$\beta_2$ (Ru) > $\beta_2$ (Zr)

$\beta_3$ (Zr) > $\beta_3$ (Ru)

Pioneering new ways to constrain neutron skin & nuclear deformation with heavy ion collisions

# Summary of nuclear structure

Haojie Xu, Chunjian Zhang, Jiangyong Jia, (STAR collab.) QM 2022

Precision ratios of flow harmonics ($v_2$, $v_3$), asymmetric cumulants (ac{3}), $\langle p_T \rangle$, moments of $\langle p_T \rangle$ fluctuation, multiplicity distribution $P(N_{ch})$ and net-charge multiplicity ($\Delta Q$) measured in isobars

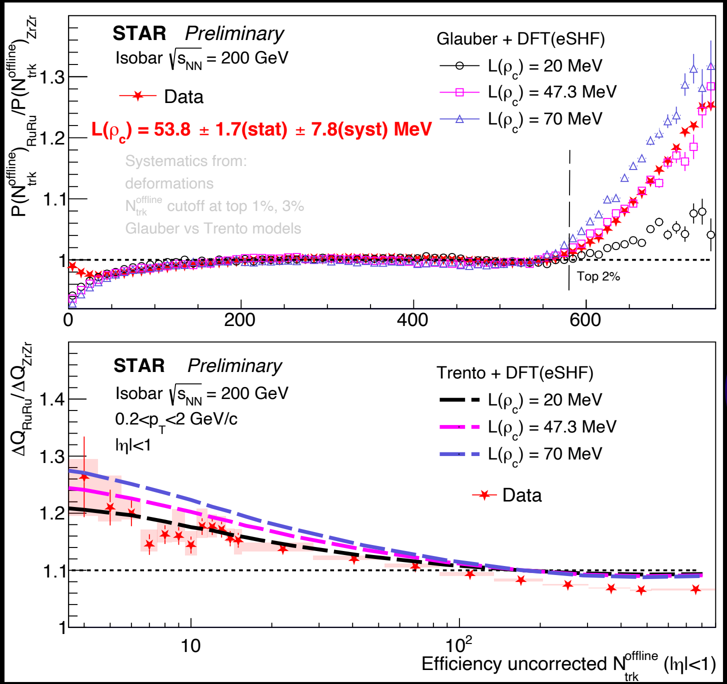


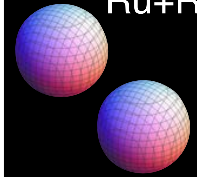

Ru+Ru

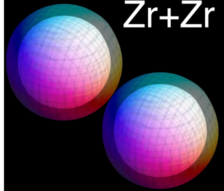

Zr+Zr

Neutron skin:
$\Delta r_{np}$ (Zr) > $\Delta r_{np}$ (Ru)

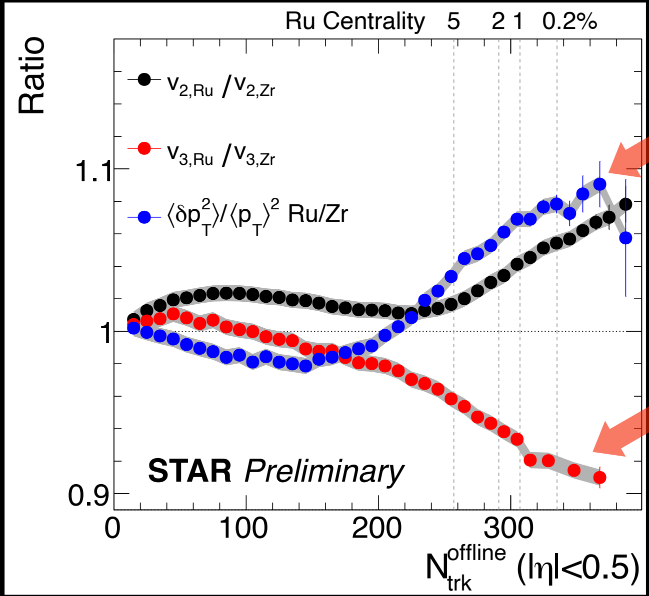


Ru+Ru

Zr+Zr

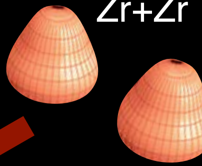

$\beta_2$ (Ru) > $\beta_2$ (Zr)

$\beta_3$ (Zr) > $\beta_3$ (Ru)

Pioneering new ways to constrain neutron skin & nuclear deformation with heavy ion collisions

# Strong field effects

# Isobar in the chart of nuclides

Elements with similar sizes but different protons so that B-field could be different

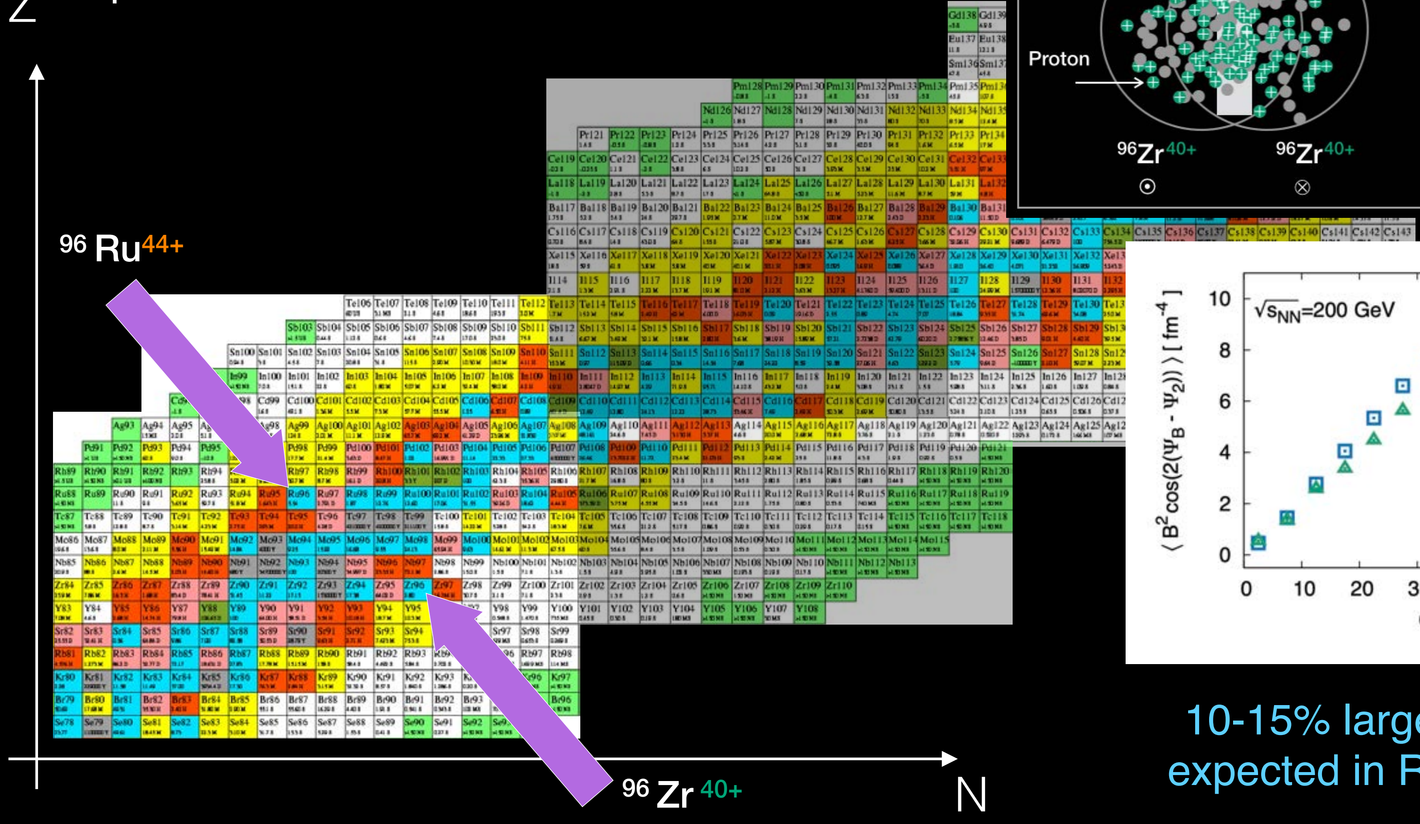


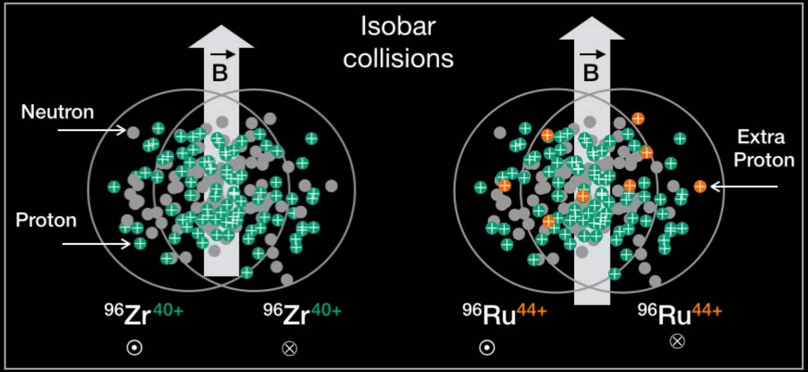


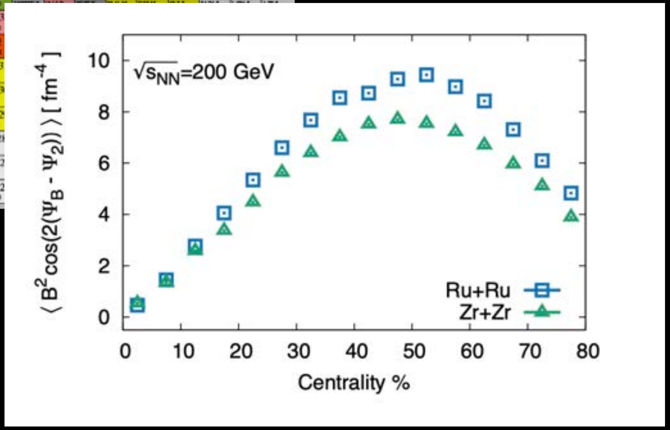


10-15% larger B-field square expected in Ru+Ru than Zr+Zr

# Independent test of B-field difference in isobars

Talk by Zhangbu Xu

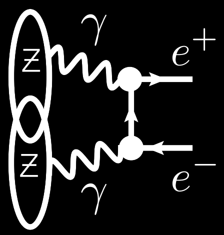


Low $p_T$ di-electron (Breit-Wheeler)

$$\sigma(\gamma\gamma \to e^+e^-) \sim \mathcal{Z}^4$$

$$\frac{\sigma_{\mathrm{Ru+Ru}}(\gamma\gamma \to e^+e^-)}{\sigma_{\mathrm{Zr+Zr}}(\gamma\gamma \to e^+e^-)} \sim \left(\frac{44}{40}\right)^4$$

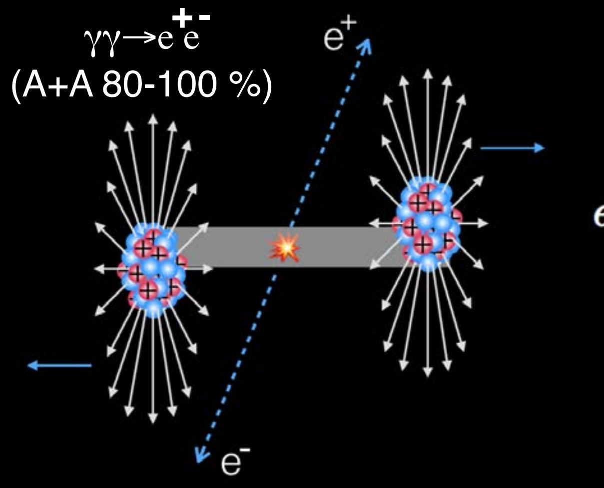


$$eB > eB_C \approx m_e^2$$

$\sim 10^{12}$ Gauss

Ru+Ru produces larger B-field than Zr+Zr

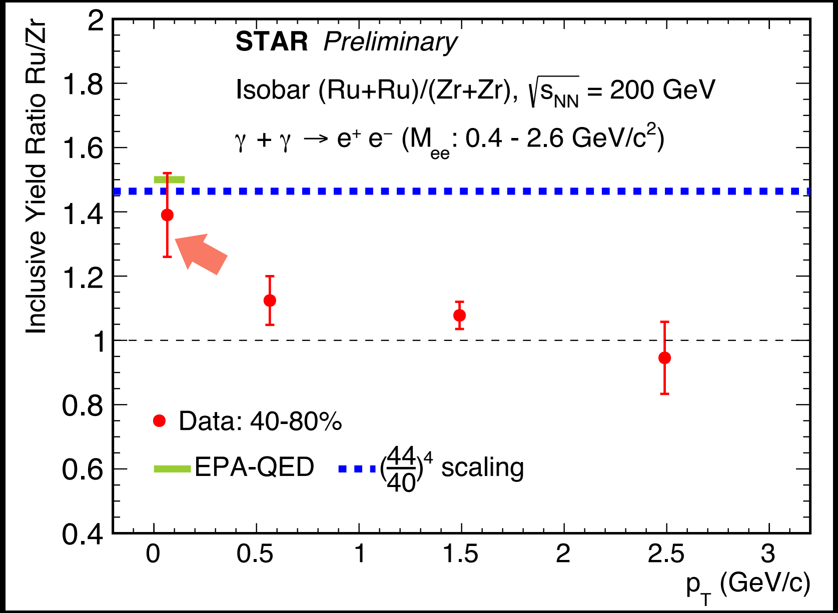


Data suggest low $p_T$ photon induced processes follow "Z" scaling of EM-fields for isobars

# Chiral Properties of the medium

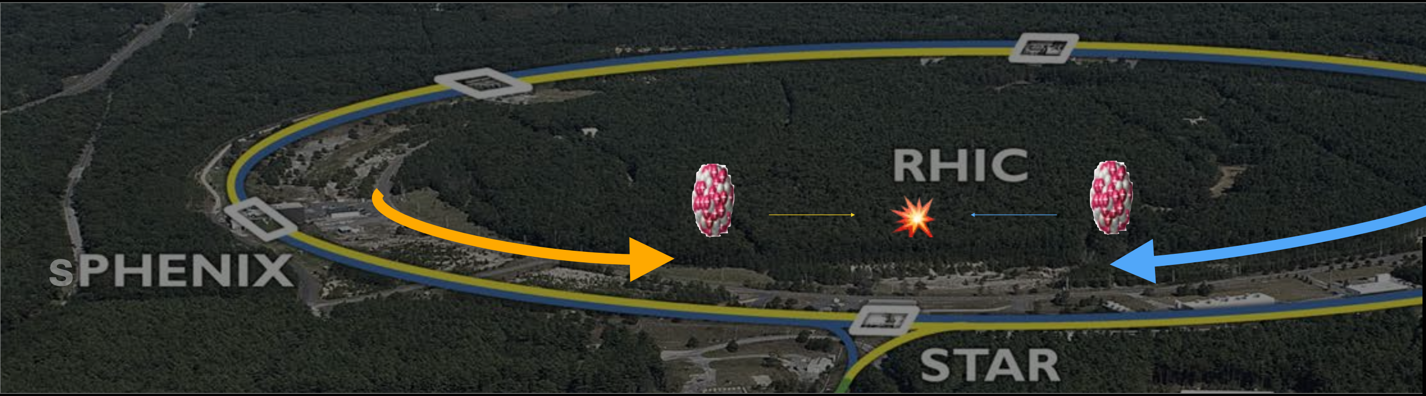


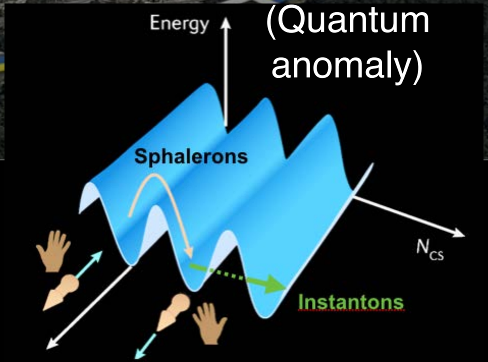


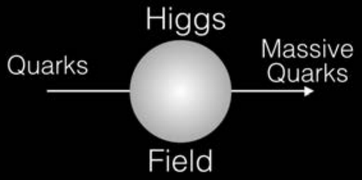


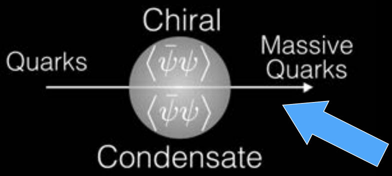


Turn this OFF

$$\mathcal{L}_{QCD} = \bar{\psi}_a \left(i(\gamma^\mu D_\mu)_{ab}\right) \psi_b - m\delta_{ab}\bar{\psi}_a\psi_b - \frac{1}{4}G^c_{\mu\nu}G^{\mu\nu}_c - \frac{\theta}{32\pi^2} g^2 F^{\mu\nu}_\alpha \tilde{F}_{\alpha\mu\nu}$$

$$= -\frac{\theta}{8\pi^2} g^2 \vec{E}_\alpha . \vec{B}_\alpha$$

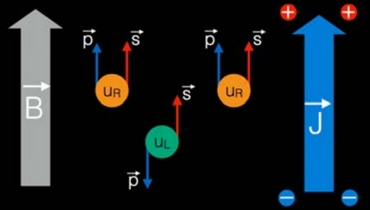


Chiral symmetry restoration ⟶ Chiral fermions

$U_A(1)$ symmetry breaking ⟶ Chirality imbalance

Strong B-field + Chirality imbalance ⟶ Chiral Magnetic Effect

# The chiral magnetic effect (CME) in four steps

**1** Deconfined medium of massless quark (chiral symmetry restored)

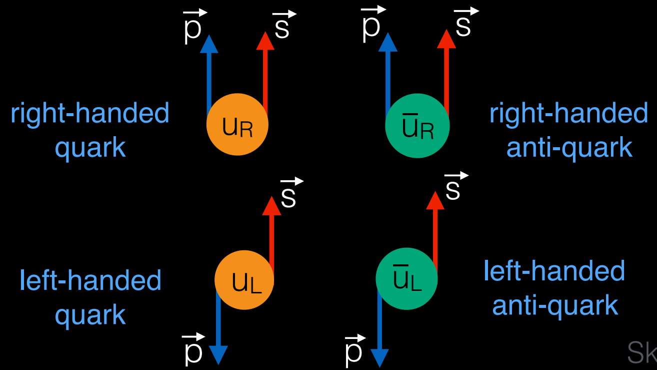


Kharzeev, McLerran,Warringa 0711.0950

**2** Mechanism to create imbalance of left & right handed quarks

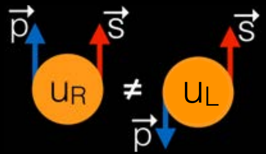


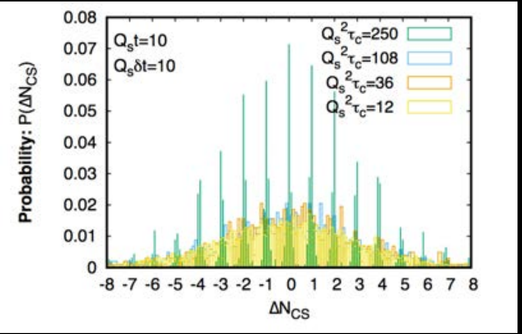


Kharzeev et al, hep-ph/0109253, Mace et al, 1601.07342, Muller et. al.1606.00342, Lappi et al,1708.08625

**3** Strong B-field

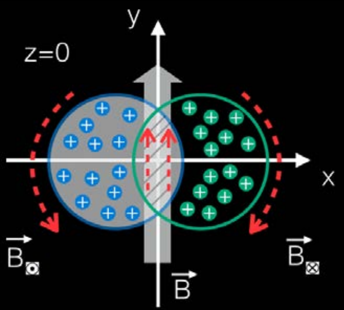


Skokov et al 0907.1396, McLerran et al 1305.0774

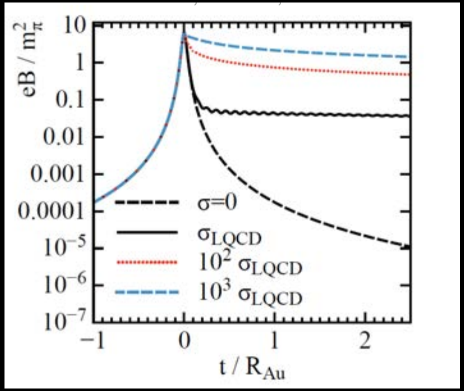


**4** The Chiral Magnetic Effect (J || B)

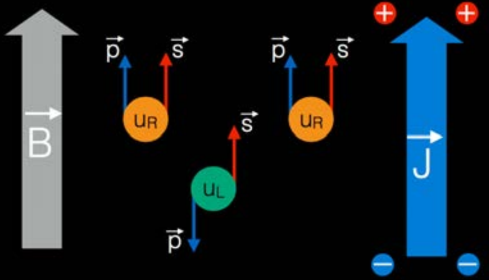


Kharzeev, arXiv:hep-ph/0406125

# How to measure charge separation due to CME ?

Measure charge separation across $\Psi_2$ using the correlator:

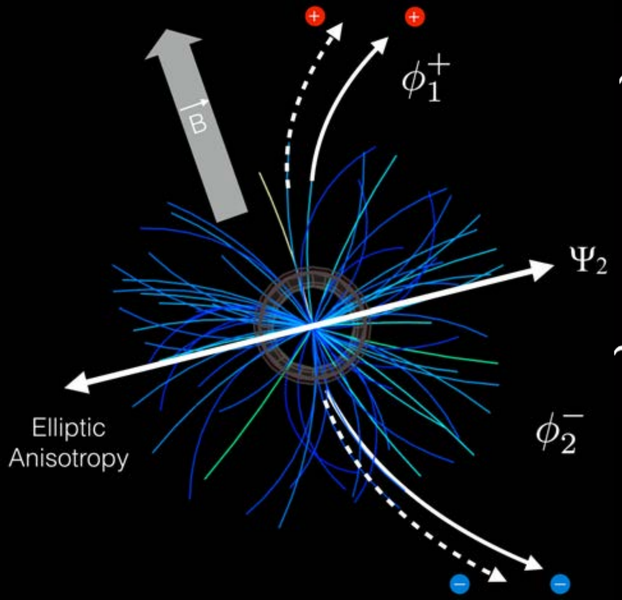


$$\gamma^{\alpha,\beta} = \langle \cos(\phi_1^\alpha + \phi_2^\beta - 2\Psi_2) \rangle$$

CME case : $\gamma^{SS} \neq \gamma^{OS}$

$$\gamma^{+-} = \cos(\pi/2 - \pi/2 + 0) = 1$$
$$\gamma^{++,--} = \cos(\pi/2 + \pi/2 + 0) = -1$$

Background:

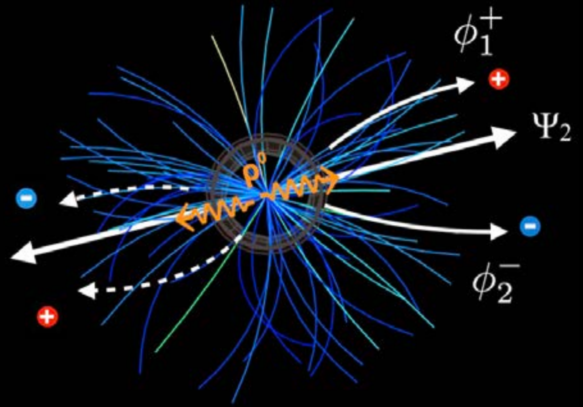


Quantity of interest:

$$\Rightarrow \Delta\gamma^{CME} = \gamma^{OS} - \gamma^{SS} > 0$$

Voloshin, hep-ph/0406311

CME causes difference in opposite-sign & same-sign correlation, background leads to indistinguishable effect

# Chiral magnetic effect search in isobar collisions

**Talk by Fuqiang Wang**

M. Abdallah et al. (STAR Collaboration), Phys. Rev. C 105 (2022) 1, 014901

Blind analysis performed with pre-defined criteria for primary CME sensitive observable:

$$\frac{(\Delta\gamma/v_2)_{\mathrm{Ru+Ru}}}{(\Delta\gamma/v_2)_{\mathrm{Zr+Zr}}} \approx 1 + f_{\mathrm{CME}}^{\mathrm{Zr+Zr}}\underbrace{[(B_{\mathrm{Ru+Ru}}/B_{\mathrm{Zr+Zr}})^2 - 1]}_{0.1\text{-}0.15} > 1 \text{ (for CME)}$$

$f_{\mathrm{CME}}^{\mathrm{Zr+Zr}}$: Unknown

Precision of 0.4% achieved

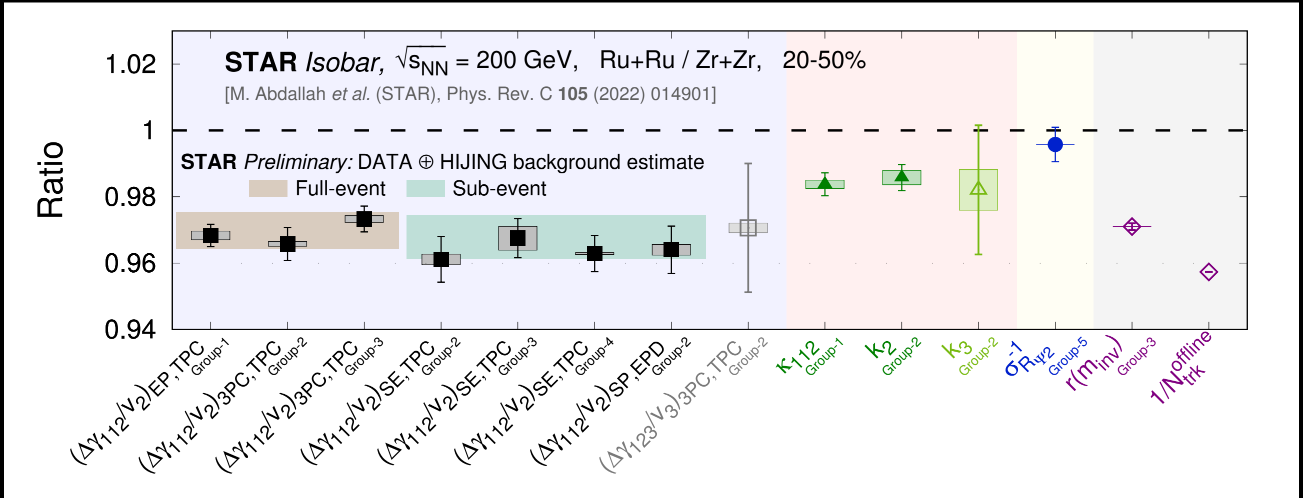


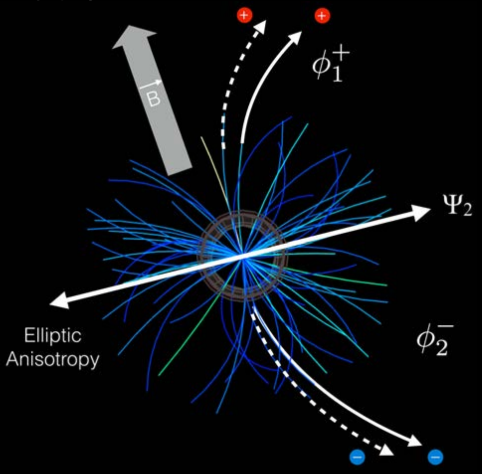


Yicheng Feng (STAR Collaboration), QM 2022

No pre-defined signature of CME is observed in isobar collisions, possible residual signal due to change of baseline & non-flow effects are under study

# Remaining signal estimates

1. STAR isobar blind analysis (most precision measurement):

M. Abdallah et al. (STAR Collaboration), Phys. Rev. C 105 (2022) 1, 014901

$$R = \frac{(\Delta\gamma/v_2)_{\mathrm{Ru+Ru}}}{(\Delta\gamma/v_2)_{\mathrm{Zr+Zr}}} = 0.9683 \pm 0.0034 \pm 0.0013$$

$$\frac{(1/N_{\mathrm{ch}})_{\mathrm{Ru+Ru}}}{(1/N_{\mathrm{ch}})_{\mathrm{Zr+Zr}}} = 0.957337 \pm 0.000017$$

2. STAR background estimate including non-flow:

Yicheng Feng, STAR collaboration, QM 2022

$$\frac{(N_{\mathrm{ch}}\,\Delta\gamma/v_2)^{\mathrm{bkg}}_{\mathrm{Ru+Ru}}}{(N_{\mathrm{ch}}\,\Delta\gamma/v_2)^{\mathrm{bkg}}_{\mathrm{Zr+Zr}}} = 1.013 \pm 0.003 \pm 0.005$$

$$R^{\mathrm{bkg}} = \frac{(\Delta\gamma/v_2)_{\mathrm{Ru+Ru}}}{(\Delta\gamma/v_2)_{\mathrm{Zr+Zr}}} = 0.9698 \pm 0.003 \pm 0.005$$

3. Estimates of Possible CME signal:

Kharzeev, Liao, Shi, 2205.00120 [nucl-th]

$$f_s = \frac{1/R^{\mathrm{bkg}} - 1/R}{\lambda_s + 1/R^{\mathrm{bkg}} - 1}$$

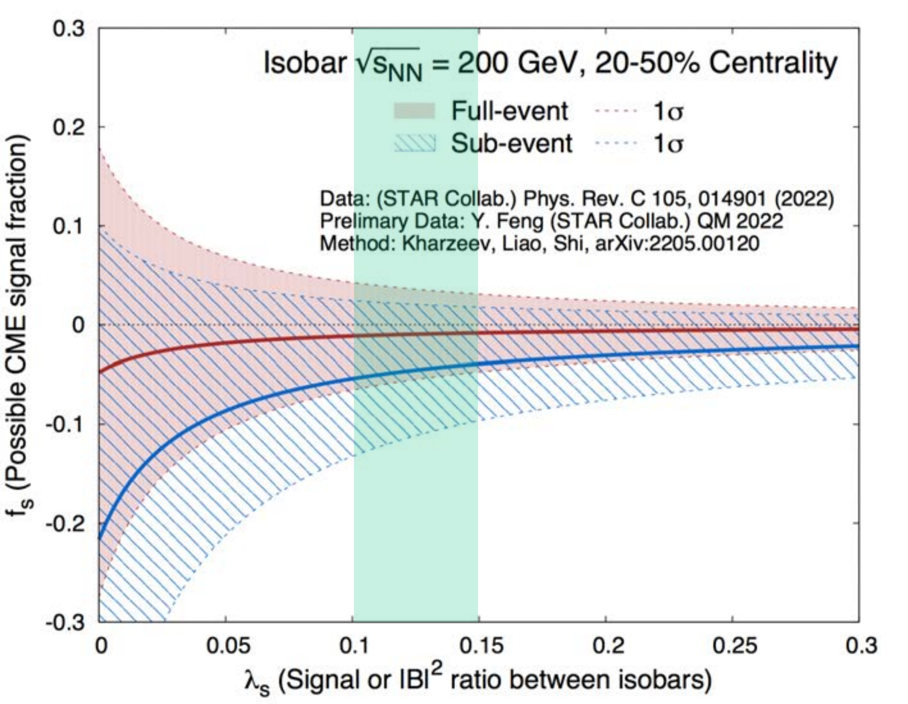


More work using the isobar data from the STAR collaboration is underway

## Study of the structure of a baryon: what carries the baryon QN?

# What carries the baryon quantum number ?

https://en.wikipedia.org/wiki/Proton
https://en.wikipedia.org/wiki/Baryon

Baryons, along with mesons, are hadrons, particles composed of quarks. Quarks have baryon numbers of $B = \frac{1}{3}$ and antiquarks have baryon numbers of $B = -\frac{1}{3}$. The term "baryon" usually refers to *triquarks*—baryons made of three quarks ($B = \frac{1}{3} + \frac{1}{3} + \frac{1}{3} = 1$).

**Proton**

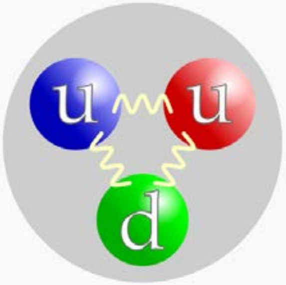


The quark content of a proton. The color assignment of individual quarks is arbitrary, but all three colors must be present. Forces between quarks are mediated by gluons.

| | |
|---|---|
| Classification | Baryon |
| Composition | 2 up quarks (u), 1 down quark (d) |
| Statistics | Fermionic |
| Family | Hadron |
| Interactions | Gravity, electromagnetic, weak, strong |

Baryon number is a strictly conserved quantum number & assumed to be carried by the quarks but never proven

G.C. Rossi and G. Veneziano, Nucl. Phys.B123(1977) 507; Phys. Rep.63(1980) 149
Kharzeev, Phys. Lett. B, 378 (1996) 238-246

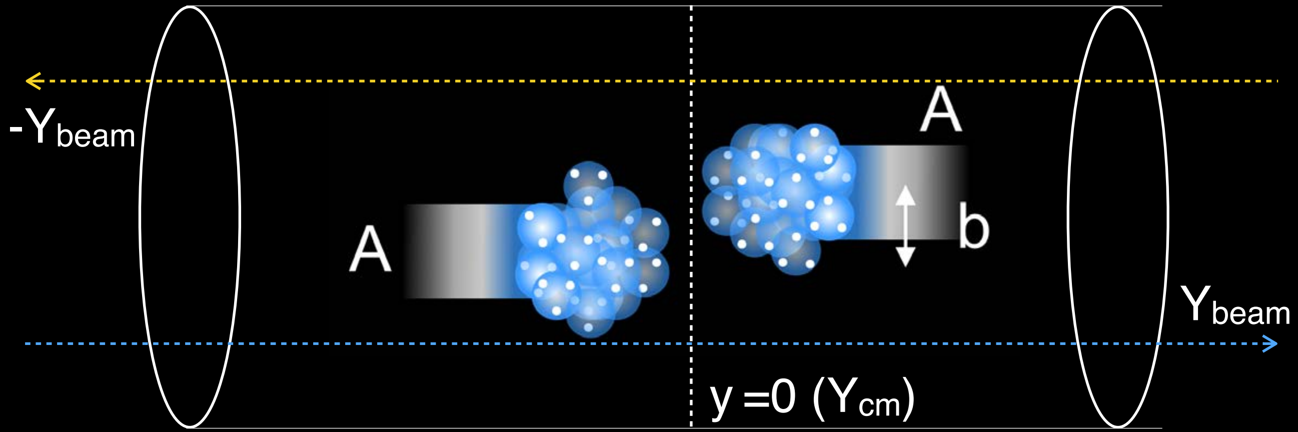


How is it stopped ? How (excess) baryons appear near the central rapidity ?

# What traces the flow of baryon quantum number ?

In the conventional picture valence traces the flow of baryon number it but this has been never prove

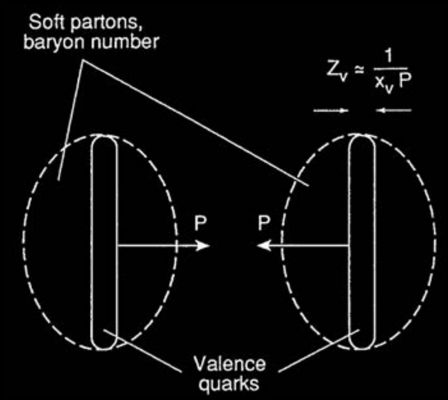


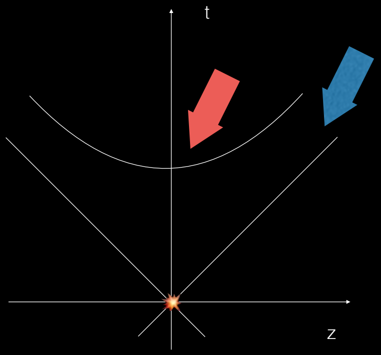


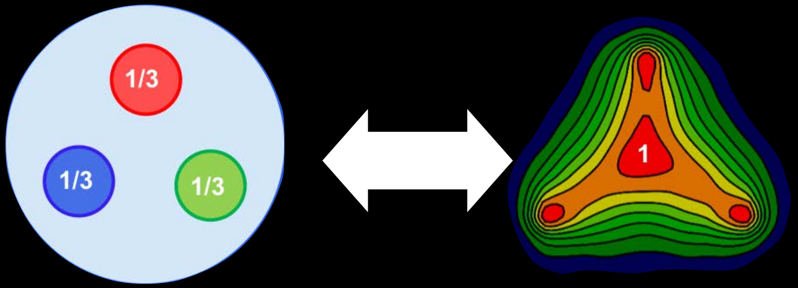


G.C. Rossi and G. Veneziano, Nucl. Phys.B123(1977) 507;
Phys. Rep.63(1980) 149
Kharzeev, Phys. Lett. B, 378 (1996) 238-246

$$t_{\rm coll} \sim (x_V P)^{-1} = (1/3 \times 100)^{-1}\ {\rm GeV}^{-1} = 0.006\ {\rm fm}$$

$$t_{\rm int} \sim \mathcal{O}(1)\ {\rm fm}$$

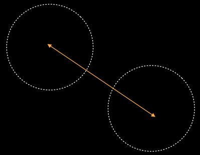

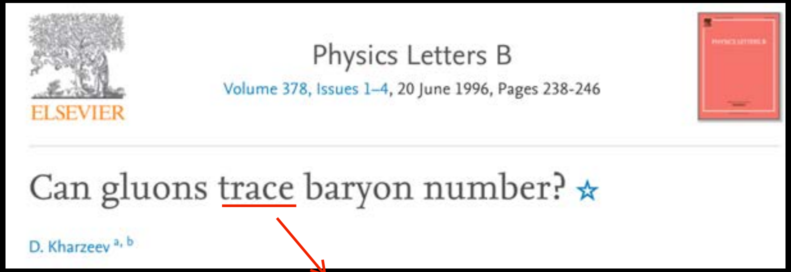
ELSEVIER
Physics Letters B
Volume 378, Issues 1–4, 20 June 1996, Pages 238-246

Can gluons trace baryon number? ☆

D. Kharzeev [a, b]

carry

The time available for valence quarks is too short to be stopped in collisions

# What trances the flow of baryon number?

G.C. Rossi and G. Veneziano, Nucl. Phys.B123(1977) 507; Phys. Rep.63(1980) 149
Kharzeev, Phys. Lett. B, 378 (1996) 238-246

Valence quarks (large-x, difficult to stop)
(trace electric charge Q & baryon number B)

String-junction of gluons (small-x, easy to stop)
(trace baryon number, quarks trace electric charge)

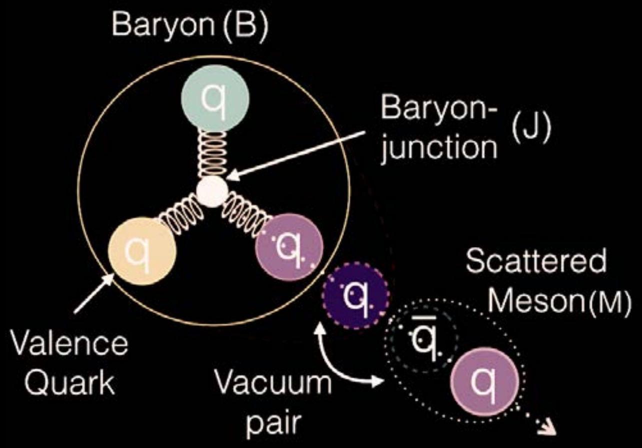


Stopping one valence quark creates a meson, stopping a baryon require stopping all three valence quarks at a fixed rapidity

Stronger y dependence for B stopping than Q stopping (less B than Q at y=0)

Stopping a junction will stop the baryon number at that rapidity, valence quarks may continue in their trajectories

Weaker y dependence for B stopping than Q stopping (equal or more B than Q at y=0)

# How a junction can be stopped?

Kharzeev, Phys. Lett. B, 378 (1996) 238-246

A string-junction from a projectile can be stopped by the soft parton field of the target and vice versa

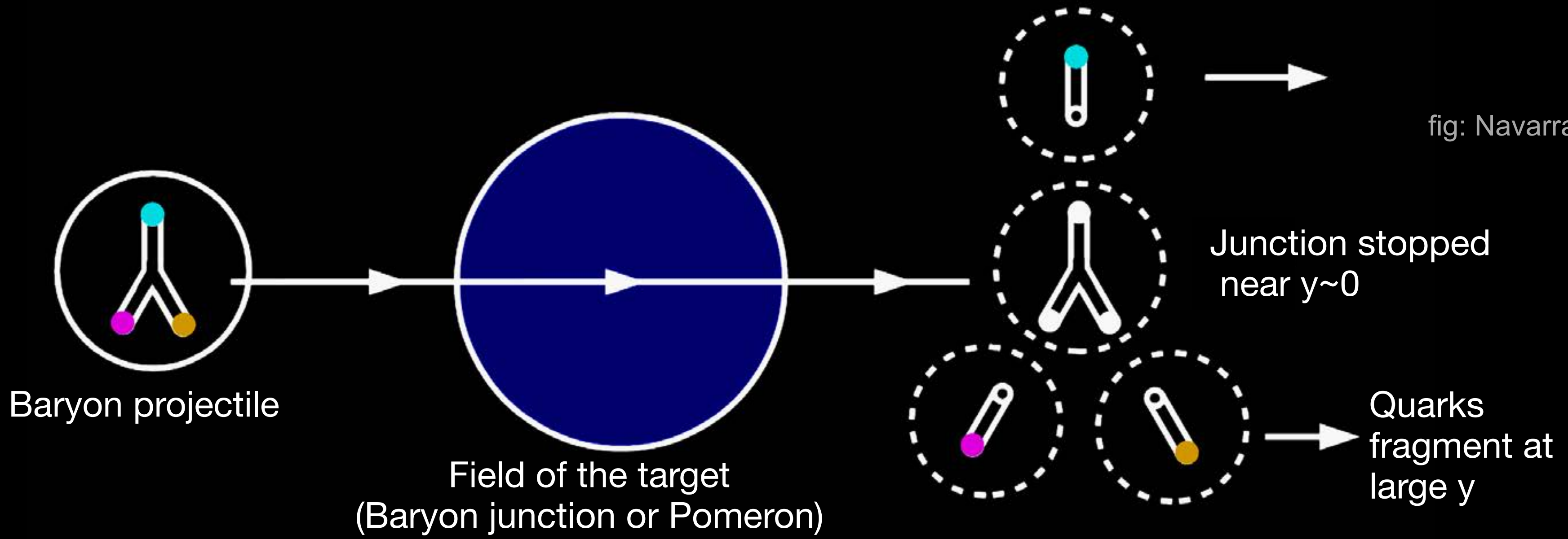


fig: Navarra

Stopped baryon will have low $p_T$ & possibly different flavor & meson production at forward y
Regge theory predicts exponential rapidity dependence for junction stopping $\sigma \sim e^{0.58(y-Y_{\mathrm{beam}})}$

# Charge vs. baryon stopping in A+A collisions

Brandenburg, Lewis, Tribedy, Xu, arXiv:2205.05685

Scenario 1: Valence quarks carry electric charge & baryon number

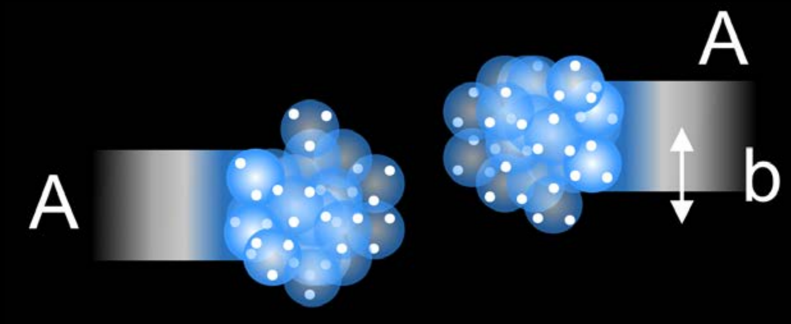


A=Mass number = Baryon number
Z=Atomic number = Electric charge

$$\text{Charge stopping} \gtrsim \frac{Z}{A} \times \text{Baryon stopping}$$

Scenario 2: Valence quarks carry electric charge & junctions cary baryon number


$$\text{Charge stopping} < \frac{Z}{A} \times \text{Baryon stopping}$$

Test if valence quarks (carry charge) & baryons are shifted to y~0 from $Y_{beam}$ in the same way

# Precision measurements in isobar collisions

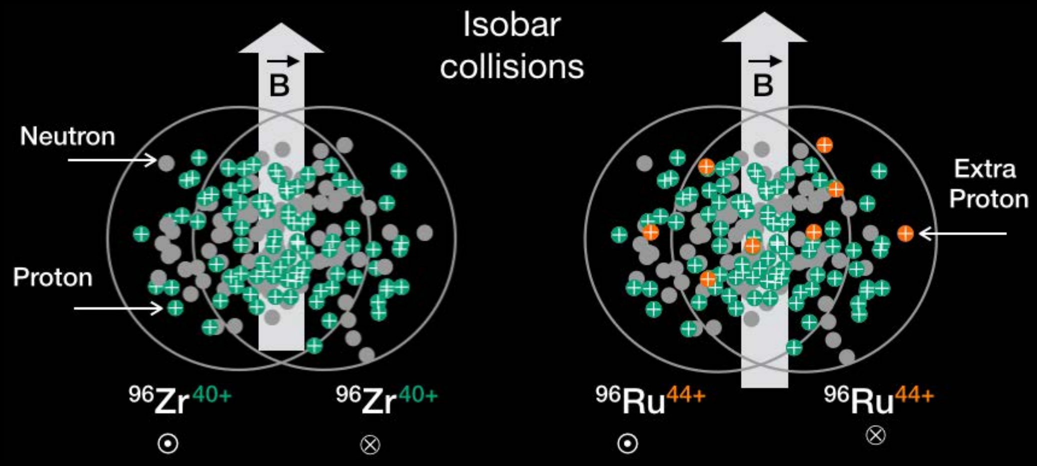


Zirconium:
A=96 (Total baryon)
Z=40 (Total charge)

Ruthenium:
A=96 (Total baryon)
Z=44 (Total charge)

Charge stopping $\Leftrightarrow$ $\frac{Z}{A}$ × Baryon stopping

Absolute charge stopping difference:

$$\Delta Q = Q^{\mathrm{Ru+Ru}} - Q^{\mathrm{Zr+Zr}}$$

Baryon stopping is same between isobars

$$B = B^{\mathrm{Ru+Ru}} = B^{\mathrm{Zr+Zr}}$$

Equivalent charge stopping difference due to baryon stopping:

$$\frac{Z^{\mathrm{Ru+Ru}} - Z^{\mathrm{Zr+Zr}}}{A} \times B$$

Goal is to test: $\Delta Q \leftrightarrow \frac{\Delta Z}{A} \times B$

The main advantage of isobar collisions is the best possible control on systematics

# How exactly isobar collision helps?



Net-baryon measurement is easy, net-charge is difficult

Isobar collision provides a way to measure the double ratios with high precision (sub-percent level):

$$R2_\pi = \frac{(N_{\pi^+}/N_{\pi^-})^{\mathrm{Ru}}}{(N_{\pi^+}/N_{\pi^-})^{\mathrm{Zr}}}$$

$$R2_K = \frac{(N_{K^+}/N_{K^-})^{\mathrm{Ru}}}{(N_{K^+}/N_{K^-})^{\mathrm{Zr}}}$$

$$R2_p = \frac{(N_p/N_{\bar{p}})^{\mathrm{Ru}}}{(N_p/N_{\bar{p}})^{\mathrm{Zr}}}$$

Net-charge stopping difference:

$$\Delta Q = N_\pi \left[ (R2_\pi - 1) + \frac{N_K}{N_\pi}(R2_K - 1) + \frac{N_p}{N_\pi}(R2_p - 1) \right]$$

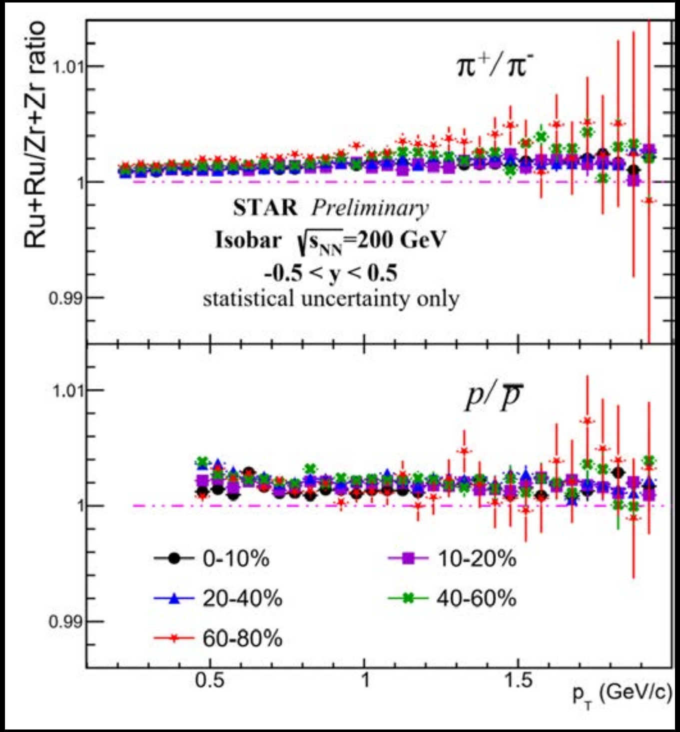


Precision net-charge measurement is extremely difficult, double ratio in isobar solves the problem

# Estimates using STAR preliminary data on isobar collisions

$$\Delta Q = N_\pi \left[ (R2_\pi - 1) + \frac{N_K}{N_\pi}(R2_K - 1) + \frac{N_p}{N_\pi}(R2_p - 1) \right]$$

Yang Li (STAR collaboration), QM 2022

$$(R2_\pi - 1) \approx (R2_p - 1) \sim 10^{-3} \quad , \; (R2_K - 1) \approx 0$$

$$\frac{N_K}{N_\pi} \approx \frac{N_p}{N_\pi} \sim 0.1$$ STAR collaboration, arXiv: 0808.2041

Absolute charge stopping difference:

$$\Delta Q \approx N_\pi \times 1.2 \times 10^{-3}$$

---

$$B \times \frac{\Delta Z}{A} = [(N_p - N_{\bar{p}}) + (N_n - N_{\bar{n}})] \times \frac{\Delta Z}{A}$$

$$\frac{N_p - N_{\bar{p}}}{N_\pi} = 0.02 \pm 0.002$$ STAR collaboration, arXiv: 0808.2041

$$\frac{N_n - N_{\bar{n}}}{N_\pi} = 1.2 \times \frac{N_p - N_{\bar{p}}}{N_\pi}$$ E864 collaboration, arXiv:nucl-ex/9909001

Equivalent charge stopping difference due to baryon stopping:

$$B \times \frac{\Delta Z}{A} \approx N_\pi \times 2 \times 10^{-3}$$

$$B \times \frac{\Delta Z}{A} = 1.6 \times \Delta Q$$

Smaller charge stopping than what is expected for same carrier of charge and baryon number

# Summary

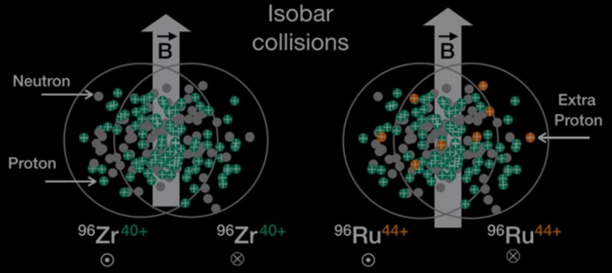


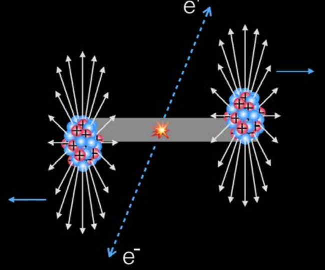


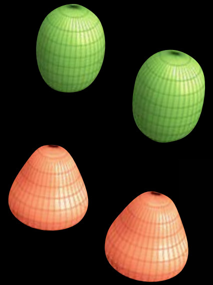

- Isobar collisions opened up path for precision measurements
- Low momentum di-lepton results already hint for B-field difference
- New opportunities to constrain nuclear shape & structure
- CME search has been narrowed down, upper limit extraction underway
- Unique opportunity to test what carries the baryon quantum number

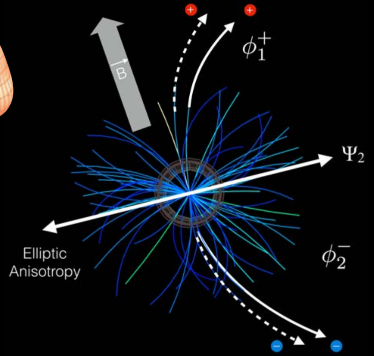


RHIC 2018 isobar was a success, the subsequent analysis of STAR data has pioneered novel measurements, the impact will go beyond heavy ion community


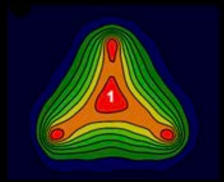

# Thank You

"For now, what is important is not finding the answer, but looking for it." — Douglas R. Hofstadter